METHOD IMPROVEMENT FOR DETERMINATION OF MICROPLASTICS IN SEAFOOD

LEUNG MING LOK

MPhil

The Hong Kong Polytechnic University

2022

The Hong Kong Polytechnic University

Department of Applied Biology and Chemical Technology

METHOD IMPROVEMENT FOR DETERMINATION OF MICROPLASTICS IN SEAFOOD

Leung Ming Lok

A thesis submitted in partial fulfilment of the requirements for the degree of

Master of Philosophy

June 2021

CERTIFICATE OF ORIGINALITY

I hereby declare that this thesis is my own work and that, to the best of my knowledge and belief, it reproduces no material previously published or written, nor material that has been accepted for the award of any other degree or diploma, except where due acknowledgement has been made in the text.

_____ (Signed)

LEUNG MING LOK (Name of student)

Abstract

Microplastics are commonly known as plastic particles < 5 mm in size. There is growing evidence showing that microplastics are increasingly abundant and associated with negative ecological consequences in marine environments. Microplastics can be easily ingested by diverse marine organisms and transferred along food chains into higher-trophic animals. Many of these animals are seafood species, raising the concern about the human health risk of microplastics through seafood consumption. There have been worldwide research efforts into the development of monitoring techniques for microplastics, but the diverse methods adopted by different researchers have made data comparison difficult among studies. Each of these approaches has its own pros and cons, which were evaluated in the present study aiming to develop an improved protocol for assessing microplastics in seafood samples.

The first part of this thesis was a literature review on recent monitoring studies of microplastics in marine mussels and fishes, two major groups of seafood. Here we summarised the findings from 50 scientific papers on this topic, from which the most common practice to extract microplastics was tissue digestion using alkaline chemicals (43%), followed by oxidative chemicals (25%), among others. About a third to a half of the tissue digestion treatments were followed by a density separation step to isolate microplastics from undigested higher-density residue such as bone fragments and sand. Almost all of these studies relied on visual inspection to manually sort microplastics (98%), which were then usually identified using Fourier-transform infrared spectroscopy (72%) or Raman spectroscopy (14%).

According to the advantages and limitations of these procedures, the second part of our work was to establish an improved protocol for assessing microplastics, using the green-lipped mussel, *Perna viridis* and the Japanese jack mackerel, *Trachurus japonicus* as the test models. A combined chemical treatment using potassium hydroxide, hydrogen peroxide and ethylenediaminetetraacetic acid disodium salt dihydrate was developed to extract microplastics from the mussel and fish samples, which achieved 99–100% digestion efficiency for both organic and inorganic biomass, and 90–100% recovery rates for seven common types of microplastics. The chemical treatment imposed only minimal effects on the particles' surface features and accuracy of polymer

identification, which showed 94–99% similarity to untreated microplastics based on Raman spectra. Another highlight was the use of an automated Raman mapping technique to minimise human handling errors in the analysis of microplastics.

The third part was about field application, in which the developed protocol was used to assess microplastics in the mariculture areas of Hong Kong. We focused on *P. viridis*, a filter-feeding mussel which can accumulate and concentrate microplastics from the ambient water. The mussel samples were collected from five sites, where the mean numbers of microplastics were determined to be 1.60–14.7 particles per individual, or 0.21–1.83 particles per g wet weight. The peak abundance of particle sizes occurred at 90–110 μm. The shapes of microplastics were dominated by fragments (89%) and fibres (9.7%). The polymer types were identified to be polypropylene (56%), polyethylene (25%), polystyrene (9.0%) and polyethylene terephthalate (10%). Through consumption of *P. viridis*, the estimated human ingestion rates of microplastics could be as high as 10,380 pieces per person per year. These findings suggest the potential human health risk of microplastics in Hong Kong and other areas in the southern China.

Overall, this thesis presented an effective digestion method for mussel and fish biomass to extract microplastics, which can be coupled with an automated Raman mapping approach to streamline the workflow of microplastic identification. Our protocol is applicable to other seafood and biological samples, providing an improved alternative for routine monitoring of microplastics in marine environments.

Publications

Leung, M. M. L., Ho, Y. W., Lee, C. H., Wang, Y., Hu, M., Kwok, K. W. H., Chua, S. L., Fang, J. K. H. (2021) Improved Raman spectroscopy-based approach to assess microplastics in seafood. *Environmental Pollution* 289, 117648 (Chapter 3 of this thesis).

Leung, M. M. L., Ho, Y. W., Maboloc, E. A., Lee, C. H., Wang, Y., Hu, M., Cheung, S. G., Fang, J. K. H. (2021) Determination of microplastics in the edible green-lipped mussel *Perna viridis* using an automated mapping technique of Raman microspectroscopy. *Journal of Hazardous Materials* 420, 126541 (Chapter 4 of this thesis).

Acknowledgements

First, I would like to express my deepest gratitude to my supervisor Dr James Kar-Hei Fang for giving me a valuable opportunity to join his team and pursue my MPhil degree. He always inspires students to think critically. During the study period, his passion for research has driven me to be more enthusiastic on my research topic. Dr Fang is a very kind and patient teacher who always emphasises the importance of learning through 'trial and error'. I deeply appreciate his attitude in research.

I would also like to express my deepest thanks to the members of our laboratory, namely Dr Samuel Cheng-Hao Lee, Dr Derek Yuen-Wa Ho, Mr Daniel Chu-Wa Mok, Mr Ryan Kar-Long Leung, Mr Ken Chue-Ho Yuen and Mr Max Wang-Tang Wong for supporting my project. Their immense knowledge always inspires me to think of different views on the same question. Moreover, I would like to acknowledge Dr Willis Sin, an engineer who has assisted me in all aspects of Raman spectrometry, particularly during the tough time at the beginning of my research. Thanks are extended to Mr John Hon-Wah Kwok and Mr Kwong-Choi Law for their assistance in fieldwork and sample collection. Without them, I wouldn't even have samples to work on.

Finally, I express my sincere gratitude to my family and all my friends. Most of my time has been spent in the laboratory in the past few years. Their understanding and care have kept me free from worry. Their great support has always cheered me up when I was exhausted. Without them, I could not have finished my degree. I would like to express my thanks to them.

Table of Contents

List of Figures and Tables

Page

Chapter 1 General Introduction

Microplastic represents a worldwide pollution problem and their numbers have been elevating over the last few decades or so. Microplastics can literally be found everywhere in aquatic environments spanning latitudes from tropical coastal waters to the remote polar oceans. The increasing microplastics are associated with ecological consequences, e.g. when ingested, causing blockage of the digestive tract of fish and in some cases mortality. Microplastics can bioaccumulate in a wide range of aquatic life, in particular bivalves which are active filter-feeders and thus more prone to uptake microplastics. Bioaccumulation allows microplastics to enter food chains and be transferred to higher trophic-level organisms. A lot of these organisms are seafood items, providing microplastics a route to the human diet. Recent research has confirmed the presence of microplastics in the human body. This is worrying but the associated human health risk is yet to be elucidated.

To track the transport, fate and risk of microplastics worldwide, a reliable and widely adopted monitoring protocol is necessary but lacking. Extraction of microplastics from environmental and biological samples commonly involves several procedures including chemical digestion to remove organic matter, isolation of microplastics from inorganic matter in a dense medium, and retrieval of the isolated microplastics on a suitable substrate prior to polymer identification using Raman spectroscopy, Fourier-transform infrared spectroscopy or other analytical techniques. Different approaches and their combinations have been used for these procedures by different researchers, discrepancy which hampers direct data comparison among studies. Moreover, each extraction approach has its own advantages, limitations and technical concerns, some of which have been confirmed to impose chemical or mechanical impacts on microplastics, or lead to particle loss and thus underestimation of the number of microplastics. These uncertainties may compromise the quality and accuracy of microplastic analysis.

In view of these situations, this thesis aimed to address major technical challenges faced in the extraction and analysis of microplastics by developing an improved protocol based on Raman spectroscopy. The test models were set to be two species of

edible mussels and fish which represent popular seafood in the Indo-Pacific region, but the developed methods are also applicable to other types of biological samples. Apart from the present General Introduction (Chapter 1), this thesis comprised a literature review on the current approaches for microplastic extraction, reported in Chapter 2, followed by two data chapters. Chapter 3 evaluated methods to streamline the workflow of microplastic extraction from seafood and that extracted microplastics were characterised using an automated Raman mapping approach. Findings from Chapter 3 allowed us to develop a protocol for the assessment of microplastics, which was applied in Chapter 4 to monitor the extent of microplastic pollution in major aquaculture zones of Hong Kong. Finally, a general conclusion was provided in Chapter 5 on the significance and other implications of this research, along with recommendations for further improvement.

Chapter 2 Recent development of the methods to assess microplastics in mussels and fishes

2.1 Introduction

Plastics are versatile materials for making numerous essentials in the 20th and 21st centuries. Other materials like woods, metals and ceramics have been progressively replaced by the plastics, owning to their properties of lightweight, toughness and cost-effectiveness (Laist, 1987). Plastics can be generally divided into two groups. Thermosoftening plastics are a group of plastics that soften when heated and can be reshaped. Examples include polypropylene (PP), polyethylene (PE), polystyrene (PS), nylon 6 (NY6), polymethyl methacrylate (PMMA), polyethylene terephthalate (PET) and polyvinyl chloride (PVC). The other group, thermosetting plastics such as polyurethane (PU), however, do not soften when heated (Table 2.1). The versatility and demand from the market confer plastic production a rapid growth rate, which has exceeded 359 million tons since 2018 and is expected to rise (Thakur et al., 2018; PlasticsEurope, 2019).

Among the various uses of plastics, packaging made of PP, PE, PS and PET account for the largest share of the market demand (> 40%; PlasticsEurope, 2019). The disposable nature of these plastic products makes them a major group of plastic waste (Andrady, 2011; Cole et al., 2011; Santos et al., 2021). Recycling can be an option to bring some plastic waste back to the production process. However, due to the heterogeneous composition of many plastic products, separation and recycling of the required polymers can be challenging (Fortelný et al., 2004). It has been estimated that 6,300 million tons of plastic waste were generated in 1950–2015, but only 9% of them were recycled (Ronkay et al., 2020). A lot of the unrecycled plastic waste ended up in landfills, or unfortunately was released into the environment. For instance, there could be over 150 million tons of plastic debris currently existing in the world's oceans (Bishop et al., 2020).

Table 2.1 Densities and chemical structures of common thermosoftening plastics and thermosetting plastics (see Stuart, 2002; Nakajima and Yamashita, 2020).

Polymer type	Abbreviation	Density (g mL^{-1})	Chemical structure
Thermosoftening plastics			
Polypropylene	PP	0.85–0.92	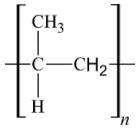
Polyethylene,	PE	0.89–0.97	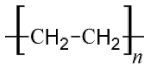
Polystyrene	PS	1.04–1.06	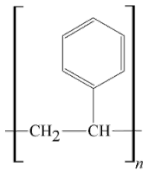
Nylon 6	NY6	1.12–1.15	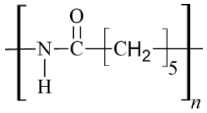
Polymethyl methacrylate	PMMA	1.16–1.20	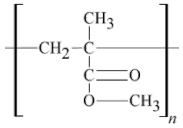
Polyethylene terephthalate	PET	1.38–1.41	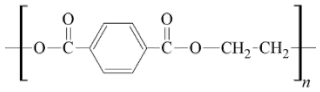
Polyvinyl chloride	PVC	1.16–1.41	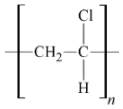
Thermosetting plastics			
Polyurethane	PU	1.20–1.26	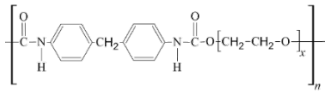

2.2 Microplastics in the environment

There are different size classes of plastic debris, among which microplastics have caught the most attention. The term "microplastics" was first used to describe plastic debris < 20 mm in a coastal pollution monitoring programme in South Africa in the 1980s (Ryan, 1990), and was later used in the United Kingdom and elsewhere as a general term for small-sized plastics (e.g. Thompson et al., 2004). Until 2009, a consensus was made in an international conference to define microplastics as plastic items < 5 mm (Arthur et al., 2009). However, this definition of "micro-" may cause confusion with the use of micrometer in the International System of Units, and

therefore some studies adopted an alternative definition of < 1,000 µm (Frias & Nash, 2019). As for the lowest size limit, to our knowledge, no consensus has been reached yet and that various values such as 0.1, 1 and 20 µm were used in the literature (Wagner et al., 2014; da Costa et al., 2016; Mendoza et al., 2018a). In the present study, the size range of microplastics is defined as 1 µm to 5 mm.

Microplastics in the environment can be categorised into primary and secondary sources. Primary microplastics are plastic particles occurring at sizes < 5 mm at the time of release. These small-sized plastics are commonly used in personal care, cosmetic and cleaning products, among others, and can be discharged along with wastewater effluents into waterways (da Costa et al., 2016; GESAMP, 2016; Napper and Thompson, 2016). Domestic washing represents another key origin of microplastics in the form of synthetic fibres, of which more than 1900 fibres can be released in a single washing cycle (Browne et al., 2011). Apart from the primary sources, microplastics can be generated from larger-sized plastics through environmental degradation and fragmentation processes. These plastic fragments, when < 5 mm, are commonly referred to as secondary microplastics (Jemec et al., 2016; Mendoza et al., 2018). The plastic degradation processes can be mechanically or biologically induced, but in the sunlit open ocean, the photochemical pathways including ultraviolet-induced oxidation and hydrolysis appear to be the dominant mechanisms (see Andrady, 2011). There is growing evidence that microplastics are increasing in abundance in the marine environment (EFSA, 2016; Chagnon et al., 2018; De Sá et al., 2018; Guzzetti et al., 2018; Waring et al., 2018).

2.2.1 Ecological impacts of plastic pollution

Plastic waste is posing a great threat to marine life by interrupting their foraging behaviour or by entanglement (Laist, 1997). For instance, up to 40,000 fur seals could be killed every year by entanglement in plastic waste (Derraik, 2002). When ingested, plastic debris can block the respiratory or digestive tract of marine animals, leading to suffocation or intestinal block which is often associated with malnutrition and decline in fitness (Tomás et al., 2002; Xanthos & Walker, 2017). Compared to larger-sized plastics, microplastics appear to be more harmful due to their greater ease to be ingested, bioaccumulated and transferred along the food chain. The presence of

microplastics has been confirmed in a wide range of marine organisms including seafood species (Li et al., 2016a; Santillo et al., 2017; Cozzolino et al., 2021). In this connection, seafood consumption represents a significant pathway for microplastics to enter human diets. Microplastics are known to cause particle toxicity as well as chemical toxicity, but the associated human health risk, where the chronic dietary exposure is of greater concern, is yet to be more clearly defined (reviewed by Verla et al., 2019).

2.2.2 Case studies of mussels and fishes

Analysis of microplastics in marine biota has largely focused on mussels and fishes worldwide, particularly on the seafood species (Alomar et al., 2021; Filgueiras et al., 2020; Li et al., 2019; Zhang et al., 2020). Previous studies have provided important information for estimating the human ingestion rates of microplastics through seafood consumption, but the various analytical approaches adopted by different researchers have hampered data comparison among studies. In this regard, this study aims to summarise the common approaches for extracting and characterising microplastics from mussels and fishes, and discuss on their advantages and limitations, providing additional information to facilitate the development of a standard protocol for microplastics. Mussels are filter feeders that continuously pump water throughout their body and capture food particles such as microalgae from the water (Beyer et al., 2017). During the filter-feeding process, mussels bioaccumulate various environmental pollutants including microplastics. The body burden of pollutants in mussels, which can be 10^4–10^5 times more concentrated than the ambient levels (e.g. Roditi et al., 2000), provides a suitable means for pollution biomonitoring of which the application has recently been extended to microplastics (Li et al., 2019). As for fishes, they are selective feeders that may not actively but mistakenly feed on microplastics, which can also be ingested through trophic transfer from their prey (Batel et al., 2016).

The present review is based on 50 research papers on microplastics in marine mussels and fishes published worldwide in 2018–2019, with the summary provided in Table 2.2. The list is not meant to be all-inclusive, but is illustrative of the recent development of the practices to extract and characterise microplastics from seafood samples.

Table 2.2 Methods reported in 50 publications in 2018–2019 to extract microplastics from mussels and fishes using dissection or digestion in hydrogen peroxide (H_2O_2), potassium hydroxide (KOH), nitric acid (HNO_3) or various enzymes at room temperature (RT) or other specified temperatures. An extra step of density separation was adopted in some studies to isolate microplastics from higher-density substances in a saturated solution of sodium chloride (NaCl), sodium iodide (NaI), potassium iodide (KI) or lithium meta-tungstate (LMT) (density = 1.2–1.6 g mL^{-1}). Extracted microplastics were characterized with visual inspection (VI), hot needles, a fluorescent tag, scanning electron microscopy (SEM), Fourier-transform infrared spectroscopy (FTIR) and Raman spectroscopy (Raman). The numbers of microplastics were expressed per unit wet weight (WW) or dry weight (DW) or per individual (Ind). The asterisks indicate extrapolated microplastics abundance from subsamples.

Mussel or fish species	Sampling area	Tissue type	Tissue digestion	Density separation	Characterisation of microplastics	Size range of quantified microplastics	Mean or median number of microplastics	Unit	Reference
Mussels									
Mytilus edulis	E coast of China	8 organ types	30% H_2O_2 at 60 °C for 48 h	NaCl	VI and FTIR	50–5000 µm	0.86–9.20	g^{-1} WW	Kolandhasamy et al. (2018)
Mytilus edulis	NE, E, SE, S, SW and W coast of UK, and supermarkets	Whole soft tissue	30% H_2O_2 at 65 °C for 24 h, then RT for 24–48 h	NaCl	VI and FTIR	8–4700 µm	0.70–1.94*	g^{-1} WW	Li et al. (2018)
Mytilus edulis	W coast of France	Whole soft tissue	10% KOH at 60 °C for 24 h	KI	VI and FTIR	20–400 µm	0.23	g^{-1} WW	Phuong et al. (2018b)
Mytilus edulis	N coast of Tunisia	Whole soft tissue	10% KOH at 65 °C for 24 h, then RT for 24–48 h	NaCl	VI and FTIR	0.05–5000 µm	0.78*	g^{-1} WW	Abidli et al. (2019)
Mytilus edulis	Fish markets in South Korea	Whole soft tissue	10% KOH at 60 °C overnight	LMT	VI and FTIR	43–4720 µm	0.12*	g^{-1} WW	Cho et al. (2019)
Mytilus edulis	NW coast of France	Whole soft tissue	10% KOH at 60 °C for 24 h	/	VI and Raman	12– >500 µm	0.15–0.25*	g^{-1} WW	Hermabessiere et al. (2019)
Mytilus edulis	SW coast of UK	Whole soft tissue	10% KOH at 70 °C for 48 h	/	VI and FTIR	Not provided	1.43–7.64*	Ind^{-1}	Scott et al. (2019)
Mytilus edulis, *M. galloprovincialis* and *M. trossulus*	NE, SE, S, SW and W coast of Norway	Whole soft tissue	10% KOH at 60 °C for 24 h	/	VI and FTIR	70–3870 µm	0.97*	g^{-1} WW	Bråte et al. (2018)

Mytilus edulis and *Perna viridis*	NE, E, SE, S and SW coast of China	Whole soft tissue	30% H_2O_2 at 65 °C for 24 h, then RT for 24–48 h	NaCl	VI and FTIR	Not provided	1.52–5.36*	g^{-1} WW	Qu et al. (2018)
Mytilus galloprovincialis	NW coast of Italy	Whole soft tissue	30% H_2O_2 at 60 °C for 1 h, then RT until clear	NaCl	VI only	Not provided	0.05	g^{-1} DW	Bonello et al. (2018)
Mytilus galloprovincialis	W coast of Greece	Whole soft tissue	30% H_2O_2 at 55–65 °C until all evaporated	/	VI and FTIR	40–737 µm	0.80*	Ind^{-1}	Digka et al. (2018a)
Mytilus galloprovincialis	W coast of Greece	Digestive gland and gills	30% H_2O_2 at 55–65 °C until all evaporated	/	VI and FTIR	<1000–5000 µm	1.83*	Ind^{-1}	Digka et al. (2018b)
Mytilus galloprovincialis	E coast of China and fish markets	Digestive gland and tract	10% KOH at 60 °C for 24 h	/	VI and FTIR	25–5000 µm	2.00–12.8	g^{-1} WW	Jin-Feng et al. (2018)
Mytilus galloprovincialis	NE coast of Italy	Whole soft tissue	Protease at 50 °C for 48 h, then 20% KOH at 50 °C for 36 h	NaI	VI and FTIR	20–300µm	0.24–1.33	g^{-1} WW	Gomiero et al. (2019)
Mytilus galloprovincialis	W coast of Italy and fish markets	Soft tissue excluding digestive gland and gills	30% H_2O_2 at 50 °C for 48 h	/	VI only	750–6000 µm	4.40–11.4*	g^{-1} WW	Renzi et al. (2018)
Mytilus trossulus	S and SW coast of Finland	Whole soft tissue	Lipase and protease at 37.5 °C for 48 h	/	VI and FTIR	20–>300 µm	0.26–0.40	g^{-1} WW	Railo et al. (2018)
Mytilus sp.	N and NW coast of Spain	Whole soft tissue	65% HNO_3 and 10% KOH, conditions not specified	/	VI only	20–5000 µm	2.30–3.44	g^{-1} WW	Reguera et al. (2019)
Mytilus spp. and *Modiolus modiolus*	N, SE and NW coast of UK	Whole soft tissue	Protease at 60 °C for 1 h	/	VI and FTIR	Not provided	0.09–3.00	g^{-1} WW	Catarino et al. (2018)
Perna canaliculus	N, NE, E, SE and W coast of New Zealand	Whole soft tissue	22.5 M HNO_3 at RT overnight, then boiled for 2 h	/	VI and FTIR	50–1000 µm	0.00–0.16	g^{-1} WW	Webb et al. (2019)
Perna perna	S coast of Brazil	Whole soft tissue	30% H_2O_2 at RT for 7 d	NaCl	VI and FTIR	Not provided	4.12–6.67	g^{-1} WW	Birnstiel et al. (2019)
Perna viridis	SE coast of India	Part of the soft tissue	By dissection only; 69% HNO_3 at RT overnight, then 6.9% at 80 °C for 2 h	/	VI and Raman	5–25 µm	0.09–2.80	g^{-1} WW	Naidu (2019)

Perna viridis	NE coast of Vietnam	Whole soft tissue	10% KOH at RT for 24 h, then 80 °C for 2 h	KI	VI and FTIR	15–400 µm	0.29	g^{-1} WW	Nam et al. (2019)
Fishes									
Acanthopagrus latus and *Konosirus punctatus*	Fish markets in China	Digestive tract and flesh	10% KOH at 60 °C for 6 h	NaCl	VI and FTIR	100–5000 µm	1.69–4.71*	Ind^{-1}	Fang et al (2019)
Acanthopagrus australis, Gerres subfascuatus and Mugil cephalus	NW coast of Australia	Digestive tract content only	Nil, by dissection	/	VI and FTIR	Not provided	0.10-2.50	Ind^{-1}	Halstead et al (2018)
Alepes djedaba, Epinephelus coioides, Platycephalus indicus, Sphyraena jello	Fishmongers in Iran	Flesh	10% KOH at 40 °C for 48 h	/	VI and hot needle	<100–5000 µm	0.57-1.85	g^{-1} WW	Akhbarizadeh et al (2018)
Boops boops	NE coast of Spain	Digestive tract content only	15% H_2O_2 at 55-65 °C until all evaporated, then 10ml 15% H_2O_2 for 48-96 h	/	VI and FTIR	<100–5000 µm	0.50-1.68*	Ind^{-1}	Garcia-Garin et al (2019)
Cheilopogon simus, *Epinephelus merra*, *Myripristis* spp. and *Siganus* spp.	W coast of French Polynesia	Digestive tract	15% H_2O_2 at 50 °C overnight	NaCl	VI only	31–2440 µm	0.15–0.39	Ind^{-1}	Garnier et al. (2019)
Engraulis encrasicolus	SW, W and NW coast of Lebanon	Digestive tract	10% KOH at 60 °C for 24 h	/	VI and Raman	<200–>1000 µm	2.50*	Ind^{-1}	Kazour et al. (2019)
Engraulis encrasicolus and *Sardina pilchardus*	S coast of France	Digestive tract content only	Nil, by dissection	/	VI and FTIR	100–4990 µm	0.11–0.20*	Ind^{-1}	Lefebvre et al. (2019)
Etmopterus spinax, *Galeus melastomus* and *Scyliorhinus canicular*	SW sea of Italy	Digestive tract	10% KOH at 60 °C overnight	/	VI and FTIR	100–5000 µm	1.18–4.47*	Ind^{-1}	Valente et al. (2019)
Evynnis cardinalis, *Inegocia japonica*, *Repomucenus richardsonii* and *Solea ovata*	S coast of China	Stomach	68% HNO_3 at 60 °C for 10 min, then RT for 24 h	/	VI and FTIR	Not provided	1.90–3.20*	Ind^{-1}	Chan et al. (2019)

Harpadon nehereus, *H. translucens* and *Sardinella gibbosa*	S coast of Bengal	Digestive tract	30% H_2O_2 at 65 °C for 24 h, then RT for 24–48 h	NaCl	VI and FTIR	<500–5000 µm	3.20–8.72*	Ind^{-1}	Hossain et al. (2019)
Merluccius bilinearis	S coast of Canada	Digestive tract content only	Nil, by dissection	/	VI and Raman	Microplastics not found	0.00	Ind^{-1}	Liboiron et al (2018)
Merluccius merluccius and *Mullus barbatus*	NE, SE and NW coast of Italy	Digestive tract	10% KOH at 60 °C for 6–12 h	/	VI, hot needle and FTIR	100–5000 µm	1.00–1.75	Ind^{-1}	Giani et al. (2019)
Mullus barbatus, *Pagellus erythrinus* and *Sardina pilchardus*	W coast of Greece	Stomach	By dissection only; 30% H_2O_2 at 55–60 °C until all evaporated	/	VI and FTIR	<100–5000 µm	0.50–0.90*	Ind^{-1}	Digka et al. (2018b)
Oncorhynchus tshawytscha	W coast of Canada	Digestive tract	10% KOH at 60 °C for 24 h	/	VI only	100–5000 µm	1.15	Ind^{-1}	Collicutt et al. (2019)
Pagellus bogaraveo and *P. erythrinus*	S coast of Italy	Digestive tract content only	Nil, by dissection	/	VI, FTIR and Raman	Not provided	/	/	Savoca et al. (2019)
Scomber colias	SW coast of Spain	Digestive tract content only	10% KOH at 60 °C for 24 h		VI and FTIR	35–5000 µm	1.78-2.55*	Ind^{-1}	Herrera et al (2019)
Zoacres viviparous	E coast of Denmark	Digestive tract	10% KOH at 40 °C for 96 h	/	VI and FTIR	400–5000 µm	NA*	/	Verlaan et al. (2019)
6 species	SW coast of Saudi Arabia	Digestive tract content only	10% KOH at RT for three weeks	/	Fluorescent tag and FTIR	125–3157 µm	0.00-1.50*	Ind^{-1}	Al-Lihaibi et al. (2019)
6 species	E coast of China	Digestive tract, gills and skin	10% KOH at 40 °C for 48 h	NaCl	VI and FTIR	27–4932 µm	13.5–22.2*	Ind^{-1}	Feng et al. (2019)
6 species	SW coast of Chile	Digestive tract	Proteinase K at 50 °C for 20 min, then 60 °C for 3 h	/	VI and FTIR	<500–5000 µm	NA*	/	Pozo et al. (2019)
11 species	East China Sea	Digestive tract and gills	10% KOH at 40 °C for 48 h	/	VI and FTIR	25–4092 µm	0.00–1.93	Ind^{-1}	Zhang et al. (2019)
11 species	A fish market in Malaysia	Viscera and gills	10% KOH at 40 °C for 72 h	NaI	VI, SEM and Raman	200–5000 µm	NA	/	Karbalaei et al. (2019)

12 species	S coast of China	Digestive tract and gills	10% KOH at 40 °C for 48–72 h	/	VI and FTIR	<250–5000 µm	0.00–14.0*	Ind^{-1}	Zhu et al. (2019a)
13 species	South China Sea	Digestive tract	69% HNO_3 at 75 °C for 24 h	/	VI and FTIR	<1000–5000 µm	0.71–4.72	Ind^{-1}	Zhu et al. (2019b)
13 species	E coast of China	Digestive tract and gills	30% H_2O_2 at 65 °C for 72 h	/	VI and FTIR	Not provided	0.30–5.30*	Ind^{-1}	Su et al. (2019)
16 species	South China Sea	Digestive tract	10% KOH at 60 °C for 7 d	$ZnCl_2$	VI, SEM and Raman	<500–5000 µm	0.00–14.0*	Ind^{-1}	Nie et al. (2019)
19 species	East China Sea	Digestive tract	68% HNO_3 at 80 °C for 1–3 h	/	VI and FTIR	16–4740 µm	0.20–0.97*	Ind^{-1}	Sun et al. (2019)
19 species	East China Sea	Digestive tract	100% HNO_3 at 80 °C for 3 h	/	VI only	Not provided	0.13–1.40	Ind^{-1}	Zhao et al. (2019)

2.3 Extraction of microplastics

Our findings show that the most widely used extraction approach was alkali digestion (43%), followed by oxidative digestion (25%; Fig. 2.1a). Among these studies, 35% and 54% of the alkali and oxidative digestion treatments, respectively, were paired with a density separation step to isolate microplastics from denser materials (Fig. 2.1b, c). Other digestion approaches using acids (13%), enzymes (6%) and mixed chemicals (2%) were less common (Fig. 2.1a). The rest of the studies did not use any digestion treatment, but relied on dissection only to extract microplastics from the digestive tract contents (11%; Fig. 2.1a). Extracted microplastics, usually in solutions, were collected on filter membranes with various pore sizes for the downstream characterisation process.

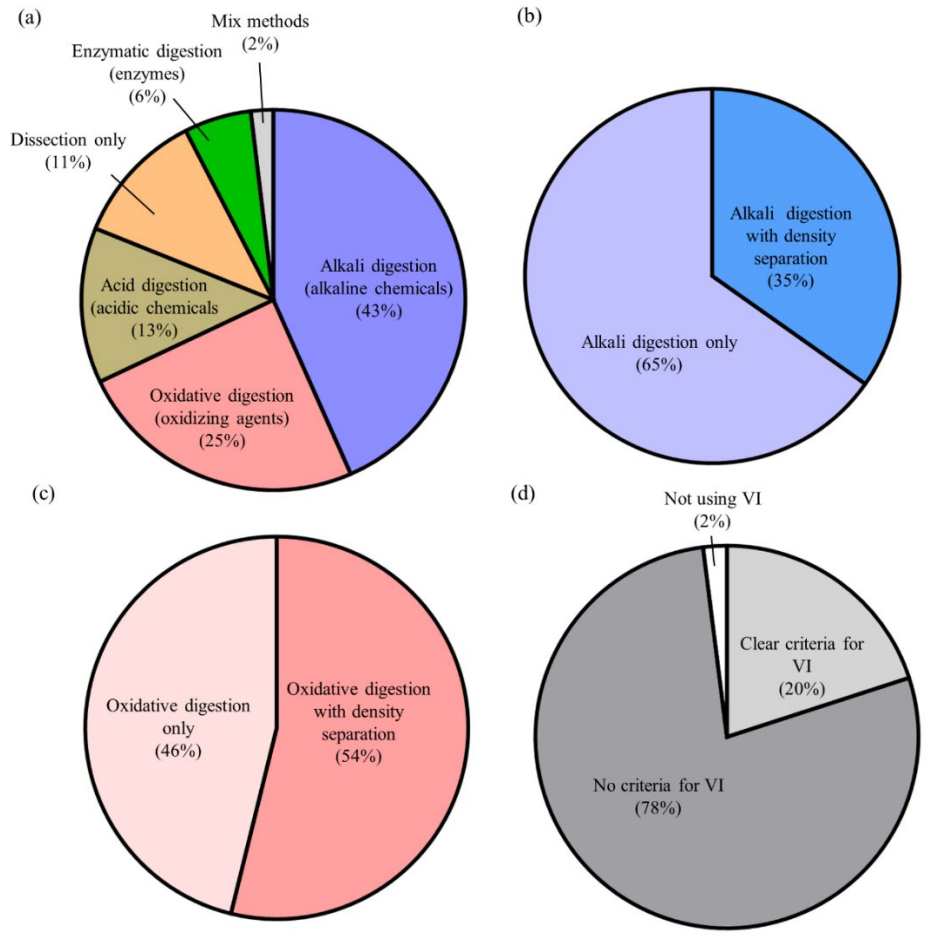

Figure 2.1 Proportions of (a) the methods used in the 50 publications (2018–2019) summarised in Table 2.2 to extract microplastics from mussels and fishes. The density separation step was used in some studies along with (b) alkali digestion and (c) oxidative digestion. (d) Most of the 50 studies relied on visual inspection (VI) but some of them did not provide clear criteria to distinguish microplastics from non-plastic particles.

2.3.1 Dissection

Microplastics can be extracted from specific organs of animals through dissection. Different body parts of marine biota including mussels and fishes have been opened to rinse out microplastics and count their numbers (Neves et al., 2015; Halstead et al., 2018; Liboiron et al., 2018; Naidu et al., 2018; Fang et al., 2019; Daniel and Thomas, 2020a). Digestive tract and gills are the two main organs targeted for this purpose to differentiate the uptake routes of microplastics via dietary exposure and waterborne exposure, respectively. The dissection approach is relatively fast and simple, allowing observation of microplastics lying on the tissue layers of specific organs, but does not capture the particles that have entered the tissues or cells or been translocated to other body parts. Previous studies showed that a substantial amount of microplastics (< 9 μm) ingested by mussels can pass through the digestive tract lining and be translocated throughout the body via circulation of haemolymph (Browne et al., 2008). This phenomenon is apparently more pronounced for smaller-sized particles. Another concern is that, by dissection, the freshly isolated microplastics are often adsorbed with body fluids or other organic matter that may interfere surface characterisation of the particles using spectroscopic means (Klein et al., 2018). In this connection, the sole use of dissection may not be ideal for extraction of microplastics, which can be facilitated by a tissue digestion step.

2.3.2 Tissue digestion

Various chemical treatments are suitable for removing the unwanted organic matter and impurities on microplastics, an issue which is commonly encountered in the dissection approach. The digestive chemicals can be alkaline, oxidative, acidic or enzymatic. With the use of these chemicals, the dissection step can often be bypassed by digesting the whole mussel or fish individuals or target organs in the first place.

2.3.2.1 Alkali digestion

Potassium hydroxide (KOH) and other alkaline chemicals can be used to digest animal tissues through hydrolysis and denaturation of proteins. The use of alkali digestion represented the most popular approach in the reviewed papers to extract microplastics from mussels and fishes (Fig. 2.1a). In particular, 10% KOH was found to be effective for digesting soft tissues of a number of marine biota (Karami et al., 2017; Xiong et al., 2018; Cho et al., 2019; Daniel and Thomas, 2020a).

The damage of KOH on microplastics was relatively mild compared to other digestive chemicals including sodium hydroxide (NaOH), nitric acid (HNO_3) and hydrochloric acid (HCl) (Cole et al., 2014; Karami et al., 2017; Thiele et al., 2019). The digestion process in KOH often requires days to weeks, but can be accelerated at an elevated temperature. The use of KOH at 40 °C has been evaluated and recommended by Karami et al. (2017), while a further increase to 60 °C was however associated with a reduced particle recovery rate of PET on which surface damage was observed.

2.3.2.2 Oxidative digestion

Hydrogen peroxide (H_2O_2) is a commonly used oxidising agent to digest organic matter for the purpose of extracting microplastics from mussels and fishes (Li et al., 2016b; Collard et al., 2017; Birnstiel et al., 2019; Bianchi et al., 2020). Tissue digestion in 30% H_2O_2 can be completed in less than a week at room temperature, but the reaction of H_2O_2 with biomass can be vigorous and associated with foam formation, in some cases leading to overflow and sample loss (Stock et al., 2019; Thiele et al., 2019). Regular check on the foam development is thus important when using H_2O_2 in tissue digestion. Nevertheless, H_2O_2 can be a good supplement to boost the digestion performance of alkaline chemicals such as KOH to extract microplastics from marine biological samples. To this end, a mixed solution of 30% H_2O_2 and 10% KOH (1:9) has been proposed for the soft tissue of oysters (Teng et al., 2019).

2.3.2.3 Acid digestion

HNO_3 is a typical chemical used in tissue digestion for numerous purposes, including extraction of microplastics from marine organisms (De Witte et al., 2014; Van Cauwenberghe and Janssen, 2014; Van Cauwenberghe et al., 2015). Complete digestion of mussel soft tissue in HNO_3 can be reached in less than 24 h, showing a higher efficiency than other digestive chemicals including HCl, NaOH and H_2O_2 (Claessens et al., 2013). Heating at more than 80 °C has been applied to further speed up the tissue digestion process to less than 2 h (Van Cauwenberghe et al., 2015; Chan et al., 2019; Mak et al., 2020). HNO_3 is certainly effective in tissue digestion, but the potential damage on microplastics should be cautioned, as the acid-treated plastics such as polypropylene and nylon 6 could be deformed, discoloured or dissolved (Karami et al., 2017; Naidoo and Glassom, 2017; Roch and Brinker, 2017).

2.3.2.4 Enzymatic digestion

Enzymes such as proteinase K can be used as a biochemical approach to break down biomass and facilitate the extraction process of microplastics. The use of enzymes is specific to particular proteins that generally does not impose damage on microplastics (Courtene-Jones et al., 2017). However, this advantage of specificity could also be a drawback, as a large volume of mixed enzymes may be required to target different proteins and other biomass to achieve complete digestion, and the use of these enzymes can incur high costs (Hurley et al., 2018; Thiele et al., 2019; von Friesen et al., 2019). Therefore, the application of enzymatic digestion may not be suitable for routine monitoring purposes. Nevertheless, enzymes can be used along with other chemical digestion methods. For instance, protease can first break down the majority of proteins, followed by KOH digestion for the remaining organics (Gomiero et al., 2019).

2.3.2.5 Density separation

The tissue digestion step is generally not effective to digest inorganic biomass such as bone fragments. This undigested biomass, and other unwanted abiotic materials such as sand particles, can be separated from microplastics using a density separation step (Birnstiel et al., 2019; Nie et al., 2019; Wakkaf et al., 2020). In brief, the particles to be separated are added into a dense medium such as solution of sodium chloride, sodium iodide, sodium tungstate or zinc chloride usually at a density of 1.2–1.5 g mL^{-1}, where lower-density microplastics float to the surface for easier collection. The major limitation of this approach is the lower applicability to higher-density plastics, such as polytetrafluoroethylene (2.2 g mL^{-1}). Another issue of the density separation step is the need for sample transfer, resuspension and retrieval of microplastics, which may increase the risk of sample loss or contamination.

2.3.2.6 Collection of microplastics from the solution

After the tissue digestion or density separation process, microplastics remained in the solution can be collected on a filter membrane in a simple filtration step, where the pore size determines the target size range of microplastics in the reported data. However, comparison of these data among studies has been complicated by the use of different pore sizes in the literature (Table 2.2). A higher number of smaller-sized microplastics can be lost when a larger pore size is used. It has been estimated that the missing smaller-sized microplastics, however, should be more abundant in

number that increases as a power function when the particle radius decreases, assuming a mass-conserving fragmentation in the environment (Lenz et al. 2016). Hence, a greater underestimation of the number of microplastics can be expected when a larger pore size is used in the extraction process.

2.4 Characterisation of microplastics

Almost all of the reviewed papers on mussels and fishes relied on visual screening to sort out suspected microplastics prior to the characterisation step, but only 20% of them provided clear criteria to define suspected microplastics (Table 2.2; Fig. 2.1d). Fourier-transform infrared (FTIR) spectroscopy was the most common technique used to characterise microplastics in these studies (72%), followed by Raman spectroscopy (14%), among others. The data of microplastics were expressed as number per unit wet weight in most of the studies on mussels (82%), but usually per individual in the papers on fishes (82%).

2.4.1 Visual assessment

Visual examination under a stereo microscope is the simplest and most popular approach to assess microplastics in terms of size, shape and number. Various criteria for identifying microplastics have been proposed for this purpose. In general, plastic materials should exhibit clear and homogeneous colour without visible cellular or organic structures and, for plastic fibres, should be equally thick throughout the entire length. Transparent or white particles, which could be easily confused with biological substances, should be more carefully examined at a high magnification (Shim et al., 2016; Qiu et al., 2016). Although visual inspection is deemed suitable for sorting out larger-sized microplastics, this approach is apparently less effective for smaller-sized particles. It has been estimated that an experienced researcher can only achieve approximate 70% accuracy to determine microplastics with size between 50–100 µm, and this accuracy is expected to be further reduced for particles < 50 µm (Directive, 2013; Lenz et al. 2015).

Another concern is that the visual approach relies on human judgement to distinguish microplastics from non-plastic particles and that the outcomes can be inconsistent. In this regard, the Nile Red staining test has been developed to facilitate visual examination. Nile Red is a fluorescent lipophilic dye that can be adsorbed on microplastics for easier observation under a fluorescence microscope

(excitation at 365 to 495 nm; Jahan et al., 2019; Dowarah et al., 2020). However, some non-plastic substances of lipophilic nature could also be stained and mistakenly counted as microplastics. An alternative approach is the hot needle test, in which a hot needle is placed near suspected microplastics, which melt or curl when heated (De Witte et al., 2014; Sathish et al., 2020). The hot needle test has been found to have low initial costs but can be a tedious process for large samples which may not be ideal for routine monitoring purposes (Lusher et al., 2017). More importantly, the approaches using Nile Red or hot needles do not provide any information about the polymer types of microplastics, a major drawback which has limited the development of these tests based on visual observation.

2.4.2 Spectroscopic approaches

The analytical instruments for polymer identification have become more affordable and increasingly available in marine laboratories. For instance, pyrolysis-gas chromatography-mass spectrometry (Pyr-GC/MS) has been utilised in research on microplastics, serving a powerful tool to determine detailed chemical compositions not only of the plastic particles but also the endogenous additives and adsorbed environmental pollutants (Hendrickson et al., 2018; Peters et al., 2018). However, specialised and highly-skilled personnel are required for the Pyr-GC/MS operation and sample preparation. Another limitation is that destructive sampling may be unavoidable, where specimens are consumed and partly destroyed during the analysis. In this connection, the non-destructive spectroscopic techniques have been more preferable. Apart from the high-end nuclear magnetic resonance spectroscopy which is not commonly accessible (Peez et al., 2019), the more user-friendly Raman spectroscopy and Fourier-transform infrared (FTIR) spectroscopy have been widely adopted in the monitoring programmes to identify and quantify microplastics in environmental and biological samples (Käppler et al., 2015; Li et al. 2019).

The biggest advantages of the Raman and FTIR techniques are clearly the simple operation and fast analytical time, which usually only require seconds to minutes for one measurement, but each of the two techniques has its own pros and cons. The Raman approach can theoretically detect microplastics as small as 1 μm, and is not affected by the presence of water or moisture in environmental and biological samples. However, acquisition of Raman spectra can be seriously interfered by the background fluorescence of biological matrices in the samples. High-performance

sample preparation is therefore necessary to remove pigments or other auto-fluorescent biomass in the samples prior to the Raman analysis (Lenz et al., 2015). In this regard, the FTIR technique provides a more cost-effective option that requires less tedious sample preparation. The use of FTIR is more suitable for larger-sized microplastics, but can be technically challenging for particles close to or smaller than 10 µm. Moreover, acquisition of FTIR spectra can be interfered by moisture and is therefore not ideal for some biological samples (Mai et al., 2018).

Nevertheless, it should be noted that the majority of studies on microplastic identification relied on FTIR spectroscopy and, as a result, it is uncommon in the literature to have monitoring data of microplastics < 10 µm (Table 2; Lenz et al. 2016; Li et al. 2019). Given the size detection limit of FTIR, and the pore size concern discussed above, the number of smaller-sized microplastics may have been underestimated in the environment.

2.4.3 The subsampling practices

The current workflow often requires the researcher to handpick suspected microplastics one by one to be manually analysed by a Raman or FTIR spectroscope. This step of particle sorting is tedious, and that subsampling has been practiced in some studies to reduce the sample processing time and effort (Nie et al., 2019; Gündoğdu et al., 2020). The subsampling and extrapolation approach is common for dissolved compounds, assuming that the concentrations are homogeneous in the samples. However, this assumption of homogeneity may not be valid for microplastics, which are a mix of particles with different densities and buoyancy. In other words, some of the particles float but some others sink, and that the estimates from a subsample may not truly reflect the situation in the whole sample. Therefore, the subsampling practice should be avoided if not necessary. In this regard, some recent studies have adopted an automated FTIR mapping technique to identify microplastics and bypass the need for manual sorting and subsampling (Bergmann et al., 2019). With the recent advances of vibrational spectroscopy, it is expected that the automated mapping function will become more common among Raman or FTIR spectroscopes, providing a useful tool to facilitate the whole-sample analysis of microplastics.

Chapter 3 Improved Raman spectroscopy-based approach to assess microplastics in seafood

3.1 Introduction

The annual global production rate of plastics has exceeded 359 million metric tons, among which 250 million metric tons may end up as waste in the ocean by 2025 (Katija et al., 2017; Plastics Europe, 2019). Plastic debris in the marine environment can be broken into microplastics, i.e. plastic pieces that are less than 5,000 μm long, through photochemical oxidation and other degradation processes (Andrady, 2011). Microplastics have raised great ecological concerns due to their increasing prevalence and harmful effects when ingested by marine organisms, such as blockage of the digestive tract, impaired predatory performance, bioaccumulation of these plastic particles and their trophic transfer along food chains (de Sá et al., 2015; Jovanović, 2017). A lot of these marine organisms are seafood items, which provide a route for microplastics to enter the human diet. There are numerous studies reporting microplastics in marine organisms, ranging from polychaetes to higher trophic-level fish including seafood species (Van Cauwenberghe et al., 2015; Collard et al., 2017; Cho et al., 2019; Hossain et al., 2020). However, the various analytical approaches and criteria adopted by different researchers have made data comparison among studies difficult (Qiu et al., 2016). Analysis of microplastics generally comprises the following four steps, each of which however holds its own limitations.

Biomass digestion – Biological samples should be digested as much as possible to extract microplastics. Otherwise, autofluorescence of the biomass would create strong interference in the analysis of microplastics using Raman spectroscopy, one of the most widely used analytical techniques in plastic polymer research (Xiong et al., 2018; Karbalaei et al., 2019; James et al., 2020). In this connection, a number of acidic solutions have been used in the biomass digestion process. However, diluted nitric acid, and probably other acids, can dissolve certain types of microplastics such as polyamine and is therefore not recommended for the analysis of microplastics (Roch and Brinker, 2017). Among other tested chemicals, diluted potassium hydroxide (KOH) appears to be more satisfactory (Avio et al., 2015a; Dehaut et al., 2016; Karami et al., 2017). The digestion effectiveness of KOH can be further boosted by the combined use with an oxidising agent such as hydrogen peroxide (H_2O_2) or sodium hypochlorite (Teng et al., 2019; Gündoğdu et al.,

2020). Despite the improved digestion efficiency, how these mixed chemicals would affect the integrity of microplastics remains uncertain. It is therefore important to assess the impacts of selected chemicals on microplastics in each biomass digestion protocol.

Density separation – The common biomass digestion protocols may not be completely effective to remove the inorganic contents in biomass such as fish bones or the mantle of bivalve shellfish (Bonello et al., 2018; Garnier et al., 2019; Bagheri et al., 2020). In this regard, a separation step in a dense medium is often used to float and separate microplastics of lower density from inorganic biomass and other abiotic matter (Claessens et al., 2013; Phuong et al., 2018; Hossain et al., 2020). The commonly used dense media include solutions of sodium chloride, sodium iodide, sodium tungstate and zinc chloride at 1.2–1.5 g mL^{-1} (Dehaut et al., 2016; Qu et al., 2018;, Karbalaei et al., 2019; Nie et al., 2019). However, these density levels are incapable of floating some of the high-density microplastics such as polytetrafluoroethylene. To address this concern, the present study explored an alternative approach using a solution of ethylenediaminetetraacetic acid (EDTA) to digest inorganic biomass and bypass the need of the density separation step. EDTA is commonly used in decalcification of bones and in this study was added in the biomass digestion step to remove both organic and inorganic contents in seafood samples (Bancroft and Gamble, 2008).

Retrieval of microplastics – Microplastics suspended in solution after the biomass digestion or density separation step are often retrieved on a filter membrane as the substrate platform to facilitate characterisation of microplastics, e.g. using Raman spectroscopy (Gündoğdu et al., 2020). The selected filter membranes should have pore sizes smaller than the target size range of microplastics, and should not generate any significant noise to the Raman signals of samples. Filter membranes made of glass fibres or cellulose esters are commonly available in marine biology and food laboratories, but these materials show strong interference in the Raman fingerprint region of plastic polymers and are thus not ideal for microplastic analysis. In this regard, we evaluated the use of filter membranes made of stainless steel, a form of iron-chromium-nickel alloys which is less sensitive to Raman excitation that may serve as a more suitable substrate for microplastic analysis.

Characterisation of microplastics – Earlier studies relied on visual inspection to identify and describe microplastics, a process that can achieve approximately 70% accuracy by trained analysts but is however prone to overestimation (Directive, 2013; Verlaan et al., 2019). The later development using Raman or Fourier-transform infrared (FTIR) spectroscopy has substantially improved the reliability of microplastic analysis, but the workflow still requires visual screening to sort out suspected microplastics to be analysed one by one. The step of visual screening is time-consuming and can be subjective and prone to handling errors. This concern can be addressed by adopting an automated mapping approach, a function that is available in some latest models of Raman or FTIR spectroscopes to locate and identify the polymer types, sizes and shapes of microplastics over a specified area on the filter substrate (Löder et al. 2015; Käppler et al. 2016; Sobhani et al., 2019, 2020; Xu et al. 2019; Levermore et al., 2020). Here, we provided an application example of using automated Raman mapping technology to streamline the workflow of microplastic analysis.

In view of the above limitations and suggested solutions, this study aimed to develop an improved protocol for assessing microplastics in seafood samples based on Raman spectroscopy. Five objectives were set to achieve this aim (Fig. 3.1). The first two objectives were centered around method optimisation: Objective 1 was to identify a filter substrate with minimal Raman interference and, while in Objective 2 we tested different chemical treatments to increase the biomass digestion efficiency, particularly for the inorganic contents which are common in marine biological samples. Objective 3 and Objective 4 were used to evaluate the effects of these digestion chemicals on microplastics in terms of particle recovery and surface modification, respectively. The developed protocol was furthermore tested in Objective 5 for its combined application with a Raman mapping approach. The evaluation was performed on two popular seafood species in the Indo-Pacific region, namely the green-lipped mussel *Perna viridis*, also a widely used species for pollution biomonitoring, and the Japanese jack mackerel *Trachurus japonicus*, which represents a commercially important fishery resource in the region (Kim et al., 2016; Sun et al., 2020).

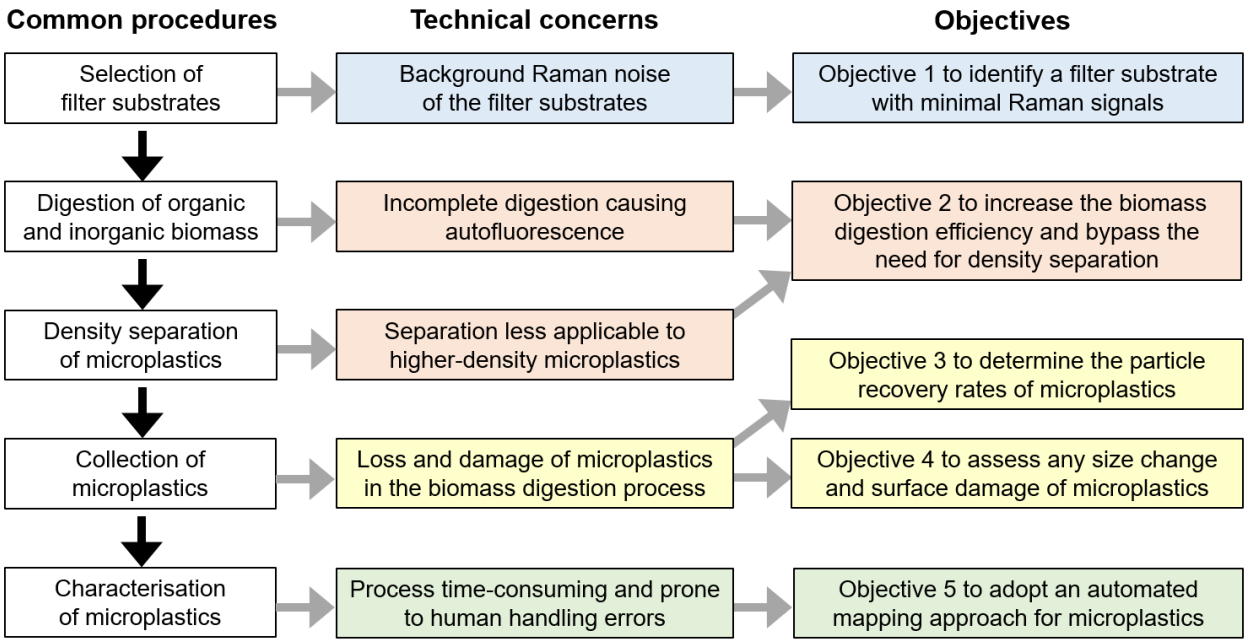

Figure 3.1 Five objectives of this study using a Raman spectroscopy-based approach to address common technical concerns in the extraction and analysis of microplastics from biological samples including seafood.

3.2 Materials and methods

Two sources of interference are common in the Raman spectroscopy-based assessment of microplastics, namely the background Raman noise due to the substrate materials, and autofluorescence due to the sample biological matrices. In this regard, the first part of this study was set to identify a type of filter substrate suitable for Raman spectrometry (Objective 1), and to develop a modified protocol to maximise the biomass digestion efficiency for *P. viridis* and *T. japonicus* (Objective 2). The two selected species are popular seafood items in the Indo-Pacific region, and contain inorganic contents (in the mussel mantle and fish bones, respectively) that are difficult to be completely digested using the common biomass digestion approaches.

3.2.1 Objective 1 to select a filter substrate suitable for Raman spectrometry

Three types of filter membranes made of glass fibres (Valusep, Thomas Scientific, Swedesboro, NJ), cellulose esters (Advantec, Tokyo, Japan) and stainless steel (Xinmingde Machinery, Henan, China) were used. Their performance as the Raman substrate was evaluated, using polystyrene (PS) of three particle sizes (300, 100 and 10 μm) as the microplastic model, in a 3 × 3 factorial experimental design leading to nine treatments (n = 5). The 300 and 100 μm PS particles were cryogenically ground from PS standard pellets (Acros Organics, Fair Lawn, NJ) using a Retsch CryoMill (Haan, Germany). The precooling stage lasted 7 min at 5 shakes s^{-1}, followed by the grinding stage for 1.5 min at 25 shakes s^{-1} at –196 °C. The ultra-low temperature was maintained by liquid nitrogen circulating outside the grinding chamber made of zirconium oxide. Ground particles of ca. 300 and 100 μm in the longest dimension were handpicked for the experiment. The 10 μm PS was supplied by Polysciences (Warrington, PA).

Five particles of each size of PS were added on each type of substrate, dried at 40 °C and assessed with a Renishaw inVia confocal Raman microspectrometer (Wotton-under Edge, UK) equipped with a Leica 10× objective (NA = 0.75; Wetzlar, Germany) and a 785 nm diode laser source (300 mW output power). Raman spectra of the PS particles were acquired in the wavenumber range of 676–1767 cm^{-1} using 10% laser power and 5 s exposure time. Baseline correction and smoothing of the acquired spectra were performed with the Renishaw WiRE 5.2 software. All sample spectra were compared to the reference Raman spectrum of PS provided in the Renishaw Polymeric Materials Database. The similarity of each sample spectrum to the reference spectrum was

indicated by the matching index provided in WiRE 5.2 (range: 0–1), an estimate which served as the tested variable among the nine treatments. A lower value of the index indicated a greater interference by the substrate material on identification of microplastics.

3.2.2 Objective 2 to assess biomass digestion efficiency

P. viridis (mussel shell length of ca. 80 mm) and *T. japonicus* (fish fork length of ca. 200 mm) were provided by local fishermen in August 2019 and stored at –20 °C. For experimental use, *P. viridis* was thawed to extract the whole soft tissue from the shells, while thawed *T. japonicus* was cut into pieces containing bones. The mussel and fish samples were blot-dried, wet-weighed and thoroughly rinsed with Milli-Q water (Merck, Darmstadt, Germany) prior to the digestion process. Sample wet weights are summarised in Table 3.1. With these biomass samples, we tested the digestion efficiency of KOH (Acros Organics) in combination with H_2O_2 (Sigma Aldrich, St. Louis, MO) and EDTA (Acros Organics). The experimental approach formed a 2 × 3 factorial design (n = 5), in which two species of biomass (*P. viridis* and *T. japonicus*) were tested across three combinations of chemicals (K, KH and KHE; Table 3.1). All solutions were prepared with Milli-Q water and filtered through 0.22 µm before use. Our goal was to develop a digestion protocol suitable for both organic and inorganic biomass including mussel mantles and fish bones

Table 3.1 Six biomass digestion treatments in objective 2 for the green-lipped mussel *Perna viridis* and the Japanese jack mackerel *Trachurus japonicus*, using three combinations of potassium hydroxide (KOH), hydrogen peroxide (H_2O_2) and ethylenediaminetetraacetic acid (EDTA). Tested biomass was measured in wet weight (mean ± SD; n = 5).

Treatment	Digestion solutions (200 mL at 40 ºC for 48 h)	Sample wet weight (g)
P. viridis		
K	200 mL 10% KOH	6.88 ± 0.73
KH	180 mL 10% KOH, added with 20 mL 30% H_2O_2	6.39 ± 0.76
KHE	180 mL 10% KOH and 14% EDTA, added with 20 mL 30% H_2O_2	6.88 ± 0.63
T. japonicus		
K	200 mL 10% KOH	4.89 ± 0.18
KH	180 mL 10% KOH, added with 20 mL 30% H_2O_2	5.30 ± 0.23
KHE	180 mL 10% KOH and 14% EDTA, added with 20 mL 30% H_2O_2	5.11 ± 0.29

The mussel and fish biomass samples were digested at 40 ºC for 48 h in treatments K, KH and KHE. The ratio of digestion volume (mL) to sample wet weight (g) was higher than 20:1. In treatment K, 200 mL of 10 % KOH was used throughout the digestion process. Treatment KH was started with 180 mL of 10 % KOH, with 10 mL of 30% H_2O_2 added twice at 24 h and 42 h to make the final volume to 200 mL. Treatment KHE was further modified from treatment KH, whose initial 180 mL solution contained 10 % KOH and 14 % EDTA. The solution after digestion was filtered through a pre-weighed filter membrane (stainless steel; pore size: 30 µm) to retain undigested biomass, if any. Each filter membrane that was coated with biomass was dried at 40 °C and reweighed. This dry weight minus the membrane pre-weight equaled the dry weight of the undigested biomass. The ratio of undigested biomass to initial biomass revealed the digestion inefficiency of each treatment, which when subtracted by one, yielded the digestion efficiency. The initial biomass was only available in wet weight and was converted into dry weight to facilitate the calculation. Additional 200 pieces of *P. viridis* soft tissue (ca. 0.6 g each) and 100 pieces of *T. japonicus* (ca. 5 g each) were blot-dried, wet-weighed, rinsed, dried at 40 °C and weighed again. The weight conversion factors for *P. viridis* and *T. japonicus* were estimated from the corresponding ratios of dry weight to wet weight.

The above work in Objective 1 and Objective 2 resolved the technical issues related to Raman interference that were caused by filter substrate and biomass materials. Treatment KHE, which used the stainless-steel filter membranes, was identified as a suitable approach to extract microplastics from the mussel and fish biomass (see Results). The second part of this study

determined how this approach would affect the characterisation of microplastics using Raman spectrometry in terms of particle recovery (Objective 3) and surface modification (Objective 4).

Table 3.2 Summary of the microplastics made by cryogenic grinding and their particle sizes, as the longest diameter (mean ± SD; n = 10).

Microplastics made	Density (g mL^{-1})*	Particle size (μm)	Plastic source
Polypropylene (PP)	0.85–0.92	566 ± 99	PP food containers
Polyethylene (PE)	0.89–0.97	601 ± 131	PE standard pellets
Polystyrene (PS)	1.04–1.09	412 ± 67	PS standard pellets
Polyamine 6/6 (PA)	1.12–1.15	508 ± 79	Nylon cable ties
Poly(methyl methacrylate) (PMMA)	1.16–1.20	535 ± 88	Acrylic sheets
Poly(ethylene terephthalate) (PET)	1.38–1.41	648 ± 125	PET egg cartons
Poly(vinyl chloride) (PVC)	1.16–1.41	564 ± 92	PVC pipes

*The values of density provided by references (Nakajima & Yamashita 2020; Stuart 2002).

3.2.3 Objective 3 to determine particle recovery rates of microplastics

Seven common types of microplastics, polypropylene (PP), polyethylene (PE), polystyrene (PS), polyamine 6/6 (PA), poly(methyl methacrylate) (PMMA), poly(ethylene terephthalate) (PET) and poly(vinyl chloride) (PVC), were used in the evaluation. The required microplastics were made with a cryogenic grinder as in Objective 1. The plastic materials were sourced from domestic products, except for PE and PS, which were standard pellets supplied by Maoming Petrochemical (Guangzhou, China) and Acros Organics, respectively. The mean particle sizes of these microplastics ranged from 412 to 648 µm (Table 3.2).

Table 3.3 Five treatments of KHE in objective 3 to evaluate the extraction recovery of microplastics from the biomass of *Perna viridis* and *Trachurus japonicus*. The spike recovery tests accounted for the background microplastics in the tested biomass. Refer to Table 3.1 for the KHE treatment conditions and Table 3.2 for the abbreviations of microplastics.

KHE digestion treatment	Spiked microplastics	Evaluation
Chemicals only + microplastics	PP, PE, PS, PA, PMMA, PET and PVC	Recovery of microplastics
P. viridis biomass	Nil	Background microplastics
P. viridis biomass + microplastics	PP, PE, PS, PA, PMMA, PET and PVC	Recovery of microplastics*
T. japonicus biomass	Nil	Background microplastics
T. japonicus biomass + microplastics	PP, PE, PS, PA, PMMA, PET and PVC	Recovery of microplastics*

*Background microplastics in the corresponding biomass to be subtracted in the calculation of recovery rates

The evaluation consisted of five treatments of KHE (Table 3.3; n = 5). In the treatment with chemicals only, ten particles of each type of microplastics (10 × 7 = 70 particles; Table 3.2) were spiked into the KHE solution and subject to the same digestion process as in Objective 2, after

which the microplastics were retrieved on a stainless-steel filter membrane (pore size: 30 µm). The numbers and polymer types of these microplastics were determined using Raman spectroscopy as in Objective 1. The recovery rate of each type of microplastics was expressed as the retrieved number to spiked number ratio.

For the other treatments with biomass, mussel and fish samples were individually homogenised with a DLAB D-160 handheld homogeniser (Beijing, China). Each homogenate was divided into two portions with similar wet weights. The seven types of microplastics were spiked into one of the portions, while the other portion served as a control to determine the background microplastics in the biomass. These pairs of spiked portion and control portion of *P. viridis* and *T. japonicus* formed the four KHE treatments with biomass (Table 3.3). Microplastics were extracted and identified from these biomass treatments, as in the chemicals-only treatment. The number of retrieved microplastics in the spiked portion, minus that in the control portion, divided by the spiked number yielded the recovery rate of each type of microplastics.

3.2.4 Objective 4 to evaluate surface modification of microplastics

Chemically-induced modification on microplastics due to treatment KHE, if any, was investigated in terms of surface damage (changes in microtopography), particle size (changes in surface area), and whether these changes would affect the accuracy of polymer identification (changes in Raman characteristic peaks).

Scanning electron microscopy was used to assess the surface microtopography of microplastics. Selected particles after treatment KHE in Objective 3, along with intact untreated microplastics, were coated with a 10–20 nm layer of gold by a Nanoimages MCM-200 ion sputter coater (Pleasanton, CA). Surface features of these microplastics, KHE-treated or untreated, were observed and compared at an acceleration voltage of 20 kV using a Tescan Vega3 scanning electron microscope (Brno, Czech Republic).

To quantify changes in surface area, the seven types of microplastics (n = 5; Table 3.2) were mounted on glass slides with an epoxy putty (Henco, Taizhou, China), a process that fixed the orientation and exposed the surface of each particle throughout the experiment. The whole slides

mounted with microplastics were immersed in the KHE solution without biomass and subject to the same digestion process as in Objective 2, before and after which the exposed surfaces of all microplastics were individually scanned at a resolution of 2 µm using a Keyence VK-X200 3D laser scanning microscope (Osaka, Japan; see Fig. 3.5a). The area of interest was set to be the exposed surface of each microplastic mounted on the epoxy putty to assess the effects of KHE. Moreover, Raman spectra were acquired from these microplastics before and after the digestion process, using the same settings as in Objective 1 in the wavenumber range of 100–3200 cm^{-1}. The similarity between the initial and final Raman peak profiles were determined based on their ratio of matching index. A lower ratio indicated a greater influence of treatment KHE on identification of microplastics.

3.2.5 Objective 5 to adopt an automated mapping approach in microplastic monitoring

Findings from Objective 3 and Objective 4 confirmed the usefulness of our improved microplastic extraction protocol, which showed > 99% digestion efficiency for biomass and > 90% recovery rates for all tested microplastics with minimal damage that can be clearly identified in Raman spectroscopy (see Results). The last part of this study was to combine this protocol with a Raman mapping approach, in which microplastics > 30 µm on a specified area were mapped and characterised by an automated programme to reduce human handling errors.

The soft tissue of *P. viridis* (n = 3) and whole fish of *T. japonicus* (n = 3), collected from the eastern waters of Hong Kong in August 2019, were digested in the KHE solution as in Objective 2. The solution after digestion was filtered through stainless-steel filter membranes with pore sizes of 250 µm (straight weave) and then 30 µm (plain Dutch weave) to separate two size ranges of microplastics, i.e. > 250 µm and 30–250 µm. Raman spectra of microplastics > 250 µm were acquired using the point-measurement approach as in Objective 1. The polymer types were identified using the Renishaw Polymeric Materials Database. Raman spectra of microplastics of 30–250 µm were acquired using an automated mapping approach, in which the whole area coated with microplastics (8 mm × 8 mm) on each filter membrane was scanned and mapped at a spatial resolution of 28.4 µm and acquisition time of 5 s per pixel. Other parameters remained the same as in Objective 1. This mapping process required approximately 14 h and produced more than 10,000 Raman spectra per sample, among which microplastics were identified using the Renishaw Polymeric Materials Database. The identified microplastics were colour-coded and illustrated in a

two-dimensional panel, from which microplastics were characterised in terms of their abundance, particle size, polymer type, and shape. The morphology of the identified microplastics was confirmed under a Cossim XTZ-7075A stereomicroscope (Beijing, China).

3.2.6 Statistical analysis

Data obtained from the factorial designed experiments in Objective 1 (3 types of filter membranes × 3 particle sizes of PS) and Objective 2 (2 species of biomass × 3 groups of chemicals in biomass digestion) were tested by two-way analysis of variance (ANOVA), in which the Raman matching index of PS and biomass digestion efficiency served as the tested variables, respectively. The data violated the Shapiro-Wilk test for normality, or homogeneity of variance, and were aligned rank-transformed using ARTool (Wobbrock et al. 2011). If interaction was significant between the two factors in two-way ANOVA, then the effect of each factor was tested by a Kruskal-Wallis test and, if significant, followed by Dunn's multiple comparisons. In Objective 4, changes in surface area were tested for each type of microplastics before and after treatment KHE using a dependent *t*-test, in which data transformation was not required. The above statistical procedures were carried out using SPSS Statistics 25.0 (IBM, Armonk, NY).

3.3 Results

3.3.1 Objective 1 to select a filter substrate suitable for Raman spectroscopy

Raman spectra of the tested filter membranes were acquired at 785 nm excitation. The glass-fibre membranes displayed a broad band that centred around 1400 cm^{-1}, while major peaks at around 900, 1300 and 1400 cm^{-1} were identified from the membranes made of cellulose esters. However, the stainless-steel membranes appeared to be insensitive to Raman excitation with no observable peaks (Fig. 3.2a). The interference of using these filter membranes as the substrate materials in Raman spectroscopy on identification of microplastics was tested with PS of three particle sizes.

The matching index, which indicated the accuracy of polymer identification, was compared among the different types of filter membranes and PS particle sizes (Fig. 3.2b–c). Significant interaction between the two factors was detected in two-way ANOVA on aligned rank-transformed data (F (4, 36) = 12.52, $p < 0.001$). The effects of filter membrane on changes in matching index of PS were then compared at each particle size class. The index values ranged from 0.86 ± 0.03 to 0.97 ± 0.07

for the 100 and 300 μm PS on different filter membranes, respectively, and no significant differences were detected among these values in respective Kruskal-Wallis tests ($p = 0.06$ and 0.37). However, when the particle size of PS decreased to 10 μm, the use of stainless-steel filter membranes resulted in significantly higher index values (0.43 ± 0.11) compared to glass fibres (0.00 ± 0.00) and cellulose esters (0.06 ± 0.13) in Kruskal-Wallis tests followed by Dunn's multiple comparisons ($p < 0.01$ and 0.05, respectively; Fig. 3.2b). Given its lower interference on PS identification, stainless steel was identified as a more suitable material of filter membranes for the Raman spectroscopy-based analysis of microplastics.

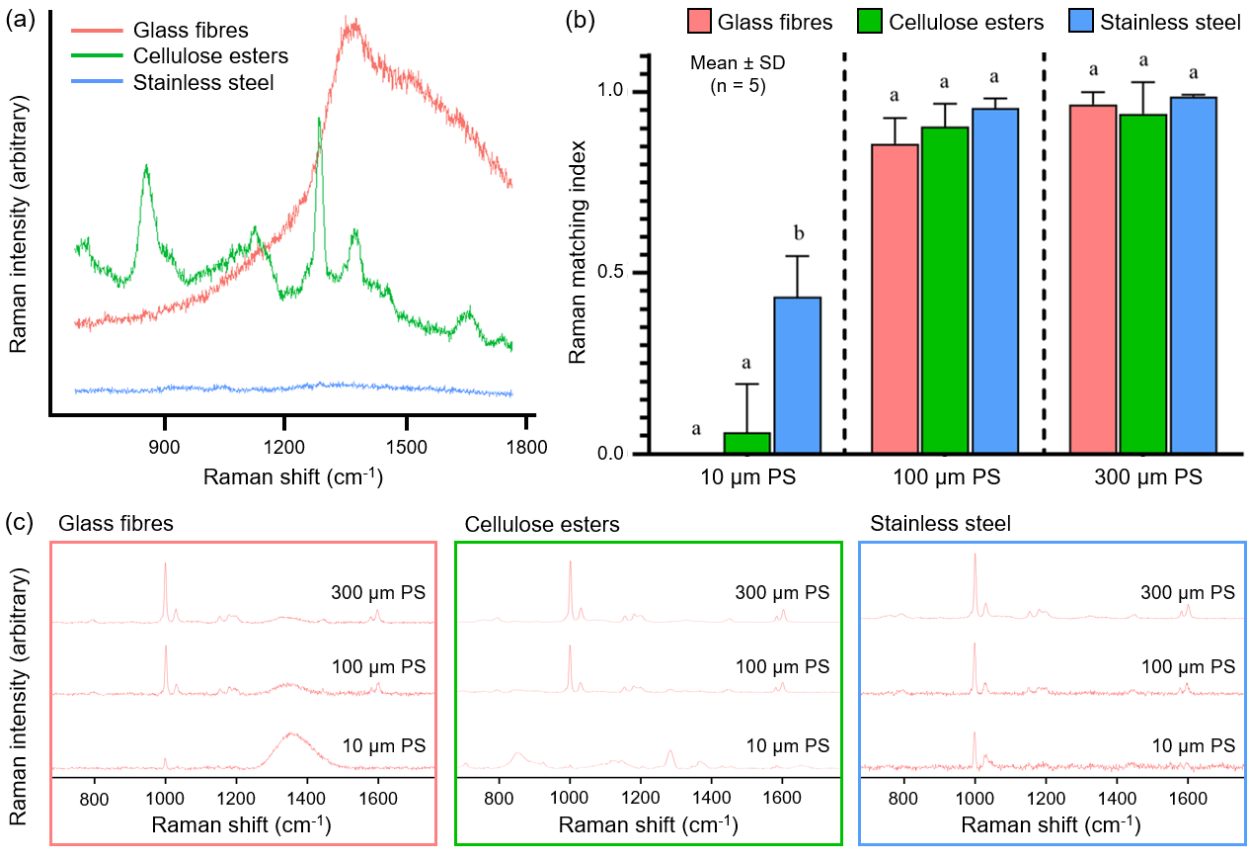

Figure 3.2 (a) Raman spectra of filter membranes made of glass fibres, cellulose esters and stainless steel excited at 785 nm; (b) Raman matching index of polystyrene (PS), determined for three particle sizes (10, 100 and 300 µm) and placed on the three types of filter membranes presented in (a). The index ranged from 0 to 1, of which a higher value indicated a greater similarity of the sample spectrum to the reference Raman spectrum. Significant interaction (filter membrane × particle size) was detected in two-way ANOVA on aligned rank-transformed data ($p < 0.05$). Kruskal-Wallis test and Dunn's multiple comparisons were used to compare the effects of filter membranes on each particle size of PS. Significant differences were detected at 10 µm PS and indicated by different lower-case letters ($p < 0.05$). (c) Raman spectra of PS of the three particle sizes placed on the three materials excited at 785 nm using a 10× objective (NA = 0.25). It should be noted that the matching index of 10 µm PS on stainless steel (0.43 ± 0.11) can be increased to 0.94 ± 0.01 (n = 5) when using a 50× objective (NA = 0.75).

3.3.2 Objective 2 to assess biomass digestion efficiency

The biomass digestion efficiency of treatments K, KH and KHE was determined on the whole soft tissue of mussels (*P. viridis*) and fish pieces with bones (*T. japonicus*) in terms of the percentage change in biomass dry weight. A significant interaction between the factors of treatment and biomass was detected in two-way ANOVA on aligned rank-transformed data (F (2, 24) = 20.742, $p < 0.001$). The effects of the three treatments were then separately compared for the mussel and

fish biomass. The digestion efficiency on mussel biomass ranged from 99.9 ± 0.13% to 100 ± 0.01%, which did not lead to any significant changes among the three treatments ($p = 0.15$, Kruskal-Wallis test; Fig. 3.3a). Although no significant changes in digestion efficiency were revealed in the calculation based on dry weight, the stereomicrographs showed a clear reduction in the amount of undigested mussel biomass in treatment KHE than that in treatments K or KH (Fig. 3.3b).

As for the fish biomass, only 74.7 ± 9.79% and 76.6 ± 6.72% were digested in treatments K and KH, respectively. A large number of undigested biomass, which was mostly fish bones, remained after the two treatments (Fig. 3.3c). Nevertheless, the fish digestion efficiency increased to 99.9 ± 0.19% in treatment KHE, which was significantly higher than that in treatment K ($p < 0.05$, Kruskal-Wallis tests followed by Dunn's multiple comparisons; Fig. 3.3a). According to these findings from mussel and fish biomass, treatment KHE was selected as a more suitable digestion method and its influence on the extraction process of microplastics was evaluated in Objectives 3 and 4.

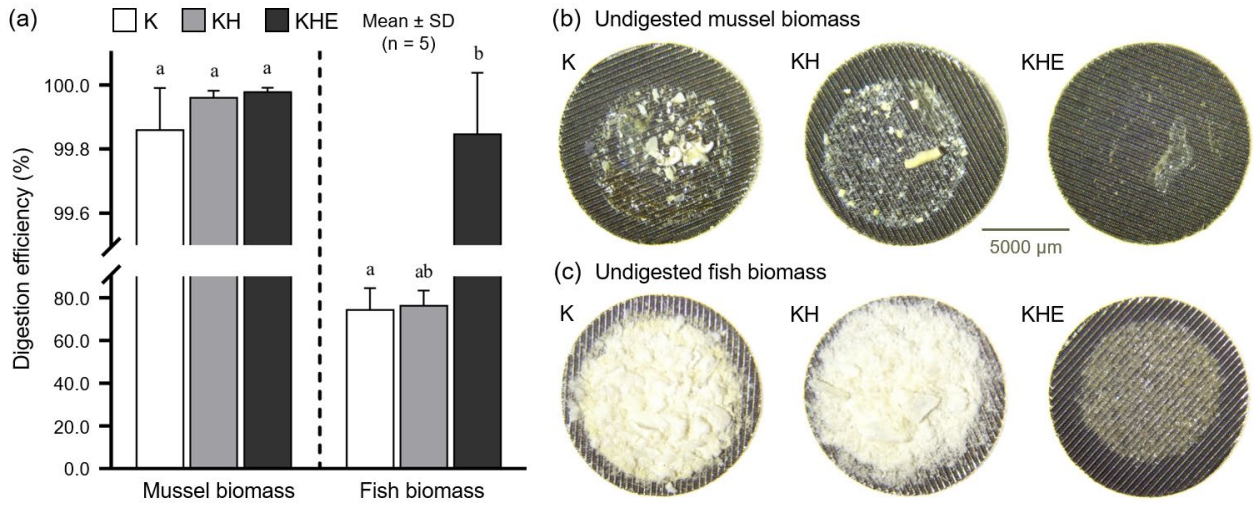

Figure 3.3 (a) Biomass digestion efficiency of *Perna viridis* and *Trachurus japonicus* in treatments K, KH and KHE. The treatment conditions are provided in Table 3.1. Significant interaction (treatment × biomass) was detected in two-way ANOVA on aligned rank-transformed data ($p < 0.05$). Kruskal-Wallis test and Dunn's multiple comparisons were used to compare the three treatments at each species of biomass. The treatment effects were found to be significant on the fish biomass, as indicated by different lower-case letters ($p < 0.05$); (b) stereomicrographs of undigested biomass of *P. viridis* and (c) *T. japonicus* retained on stainless-steel filter membranes (pore size: 30 µm) after treatments K, KH and KHE. All panels in (b) and (c) share the same scale bar.

3.3.3 Objective 3 to determine particle recovery rates of microplastics

Seven types of microplastics were spiked in treatment KHE with and without biomass, after which the spiked particles were retrieved on stainless-steel filter membranes and identified based on Raman spectra (Fig. 3.4). It was confirmed that the tested biomass did not contain any background microplastics. The spike recovery rates of microplastics were summarised in Table 3.4, of which the mean values in the chemical-only treatment (90–100%) were similar to those with the mussel biomass (92–100%) and fish biomass (90–98%). These findings showed the effectiveness of treatment KHE to extract microplastics from biomass in terms of particle number.

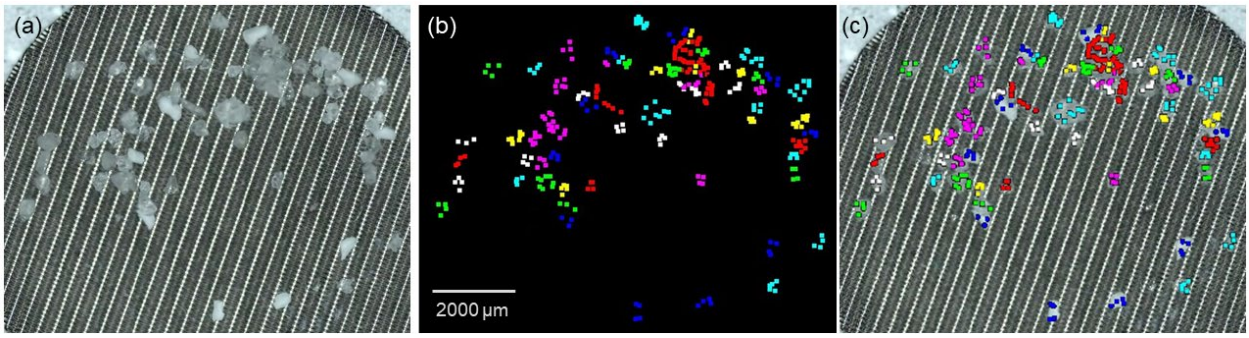

Figure 3.4 (a) Microplastics retrieved on a stainless-steel filter membrane after the spike recovery test, (b) their identification using Raman spectroscopy in a point acquisition mode at 785 nm excitation, and (c) the superimposed image of (a) and (b). Retrieved microplastics were counted and identified to be PP (purple), PE (cyan), PS (yellow), PA (white), PMMA (green), PET (red) and PVC (blue). Refer to Table 3.2 for the abbreviations of microplastics. The coloured dots indicate the acquisition points of Raman spectra. Three or four spectra were acquired for each particle to verify the polymer type.

Table 3.4 Spike recovery rates (%) of microplastics in treatment KHE with and without biomass of *Perna viridis* and *Trachurus japonicus* (mean ± SD; n = 5). Refer to Table 3.1 for the KHE treatment conditions and Table 3.2 for the abbreviations of microplastics.

Treatment KHE	PP	PE	PS	PA	PMMA	PET	PVC
Chemicals only	100 ± 0.00	96.0 ± 5.48	98.0 ± 4.47	100 ± 0.00	96.0 ± 5.48	96.0 ± 5.48	90 ± 7.07
P. viridis biomass	94.0 ± 8.94	92.0 ± 4.47	96.0 ± 5.48	100 ± 0.00	98.0 ± 8.37	100 ± 0.00	96.0 ± 5.48
T. japonicus biomass	98.0 ± 8.37	96.0 ± 5.48	90.0 ± 7.07	96.0 ± 5.48	96.0 ± 5.48	96.0 ± 5.48	96.0 ± 5.48

3.3.4 Objective 4 to evaluate surface modification of microplastics

Changes in surface area of microplastics due to treatment KHE were evaluated using 3D laser scanning technology (Fig. 3.5a). No significant changes were found in all types of microplastics except PP and PVC, of which the mean surface areas significantly increased by 16.2 ± 6.64% and 7.86 ± 4.03% after the treatment, respectively ($p < 0.05$, dependent *t*-test; Fig. 3.5b). Likewise, the scanning electron micrographs displayed similar microtopography between the KHE-treated and untreated microplastics, but slightly more peeling was observed on some particles including PP after the treatment. Another observation was that the treated PVC was associated with crevices and pits on the surface (Fig. 3.6). Raman spectra of the microplastics were compared before and after treatment KHE. The spectra of all pairs were almost identical, reaching a similarity of 94–99% which revealed the minimal effect of treatment KHE on the accuracy of identifying microplastics despite the surface modification on PP and PVC (Fig. 3.7; Table 3.5).

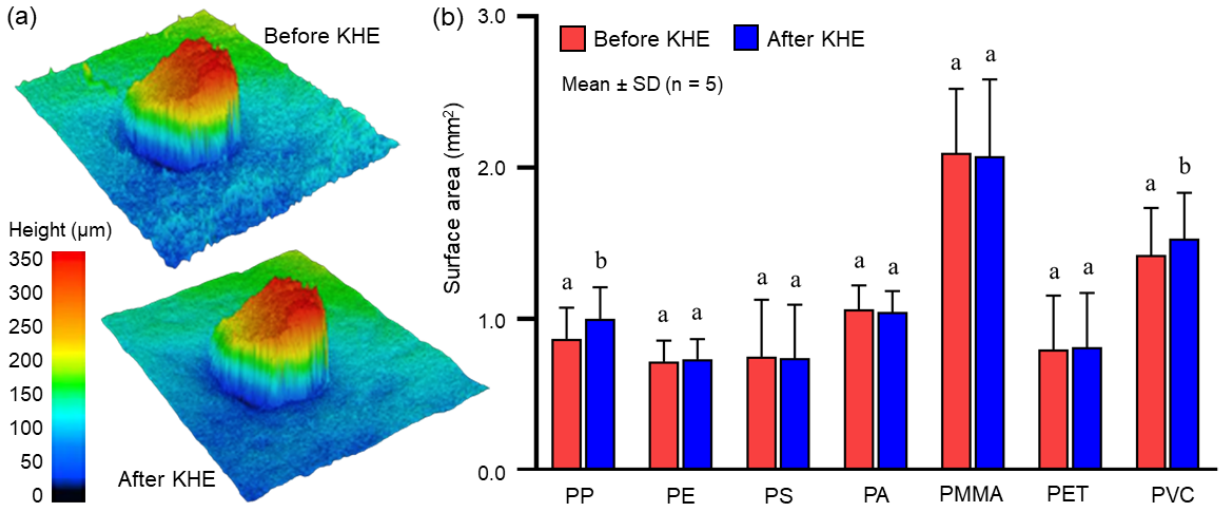

Figure 3.5 (a) The surface area of a representative microplastic measured at a resolution of 2 µm using 3D laser scanning technology, before and after treatment KHE (see Table 3.1). The substrate layer was an epoxy putty to mount the microplastic on a glass slide; (b) changes in surface area of microplastics due to treatment KHE, determined as in (a). Significant increases were detected for PP and PVC in respective dependent *t*-tests, and indicated by letters a and b ($p < 0.05$). Refer to Table 3.2 for the abbreviations of microplastics.

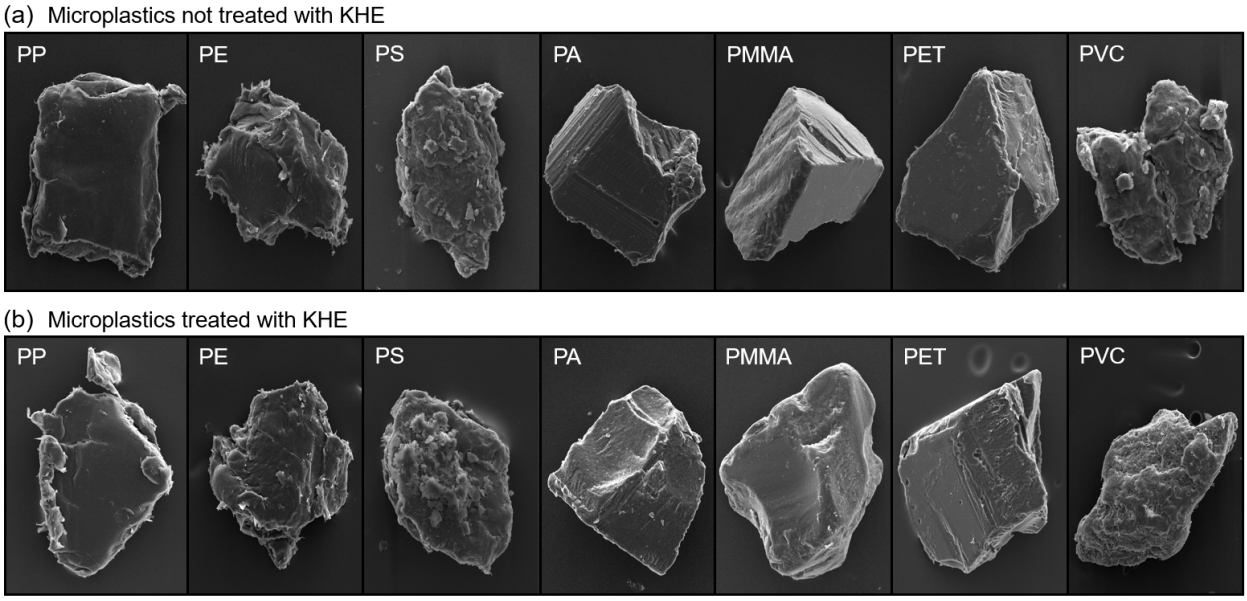

Figure 3.6 Scanning electron micrographs of representative microplastics (a) not treated with KHE and (b) treated with KHE. The micrographs presented in (a) and (b) were produce from different particles. Sizes of the displayed particles were ca. 200–500 µm. Refer to Table 3.1 for the KHE treatment conditions and Table 3.2 for the abbreviations of microplastics.

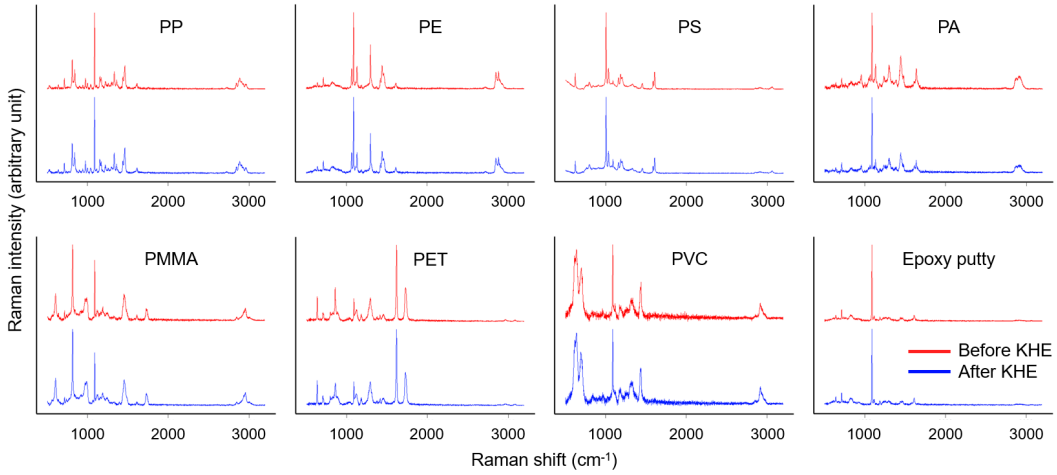

Figure 3.7 Raman spectra of microplastics, and the epoxy putty used to mount microplastics (see Fig. 3.5), before and after treatment KHE (see Table 3.1). Raman spectra were acquired at 785 nm excitation. Refer to Table 3.2 for the abbreviations of microplastics.

Table 3.5 Similarity (%) between the Raman spectra of microplastics before and after treatment KHE reported in Fig. 3.7, as indicated by the ratio of matching index (mean ± SD; n = 5). Refer to Table 3.2 for the abbreviations of microplastics.

PP	PE	PS	PA	PET	PMMA	PVC
98.8 ± 1.79	94.4 ± 3.91	93.8 ± 3.77	95.2 ± 3.49	99.0 ± 0.71	99.0 ± 1.00	95.2 ± 4.55

3.3.5 Objective 5 to adopt an automated mapping approach in microplastic monitoring

The improved extraction method for microplastics using stainless-steel filter membranes and treatment KHE was combined with a Raman mapping technique to characterise microplastics in seafood samples (Fig. 3.8). *P. viridis* and *T. japonicus* were used in this evaluation, where 32.7 ± 29.3 and 8.33 ± 7.09 pieces of microplastics per individual were found in the mussel soft tissue and whole fish, respectively (Fig.3. 9a), values that were equivalent to 4.46 ± 3.72 and 0.26 ± 0.16 per g wet weight in the mussels and fish. The particle size ranges of the identified microplastics were 38.2–820 µm and 67.7–805 µm, respectively, in the mussels and fish in terms of the longest dimension (Fig. 3.9a).

The microplastics were dominated by fragments, accounting for 97.6% and 80.0% in the mussels and fish, respectively, followed by fibres (Fig. 3.9b, 3.10). As for the polymer types, 82.7% of the microplastics extracted from mussels were confirmed to be PP, followed by PE (16.3%) and PET (1.02%). The highest proportion of PP (32.0%) was also found among the microplastics in fish, of which the polymer types were more diverse also including PS (28.0%), PE (24.0%), PET (12.0%) and PMMA (4.00%; Fig. 3.9c). These findings confirmed the presence of microplastics in seafood in Hong Kong.

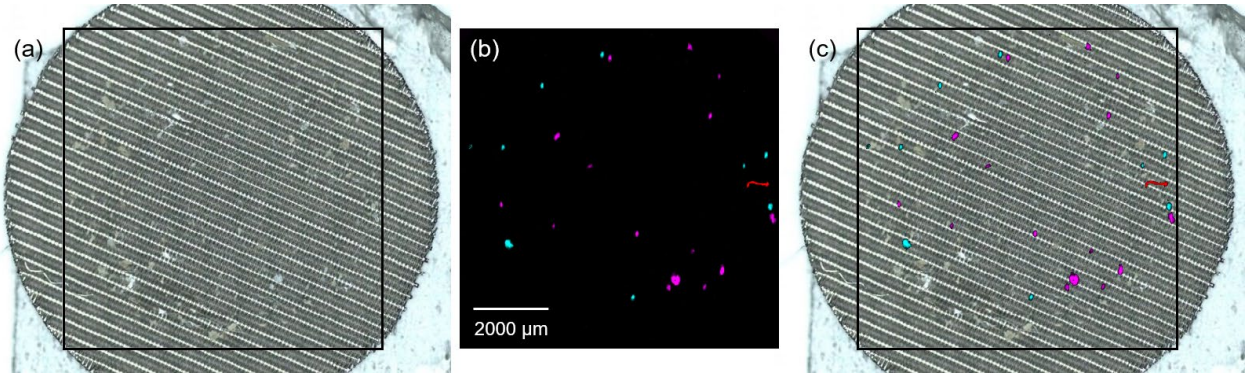

Figure 3.8 (a) Microplastics on a stainless-steel filter membrane, (b) their colour-coded identification using an automated Raman mapping approach, and (c) the superimposed image of (a) and (b). All particles including microplastics within the black square were scanned and mapped at a spatial resolution of 28.4 µm, where polypropylene (pink), polyethylene (cyan) and poly(ethylene terephthalate) (red) were found in this sample.

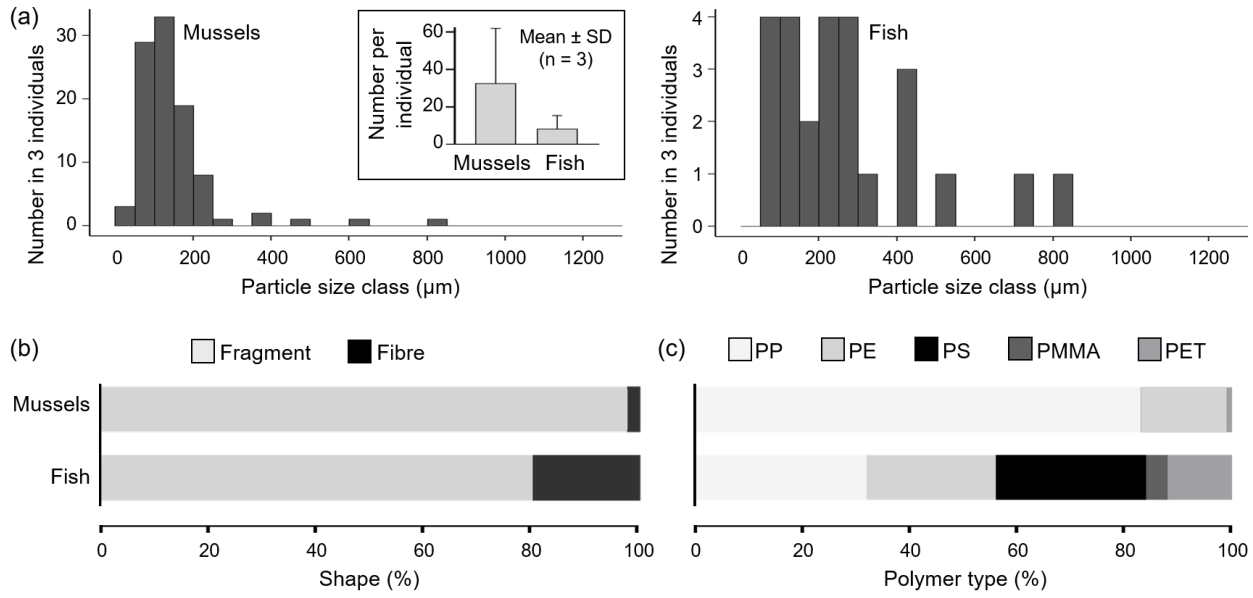

Figure 3.9 (a) Number and particle size range of microplastics identified in *Perna viridis* (ca. 80 mm shell length) and *Trachurus japonicus* (ca. 200 mm total length), and the proportional distribution of microplastics in terms of (b) shape and (c) polymer type.

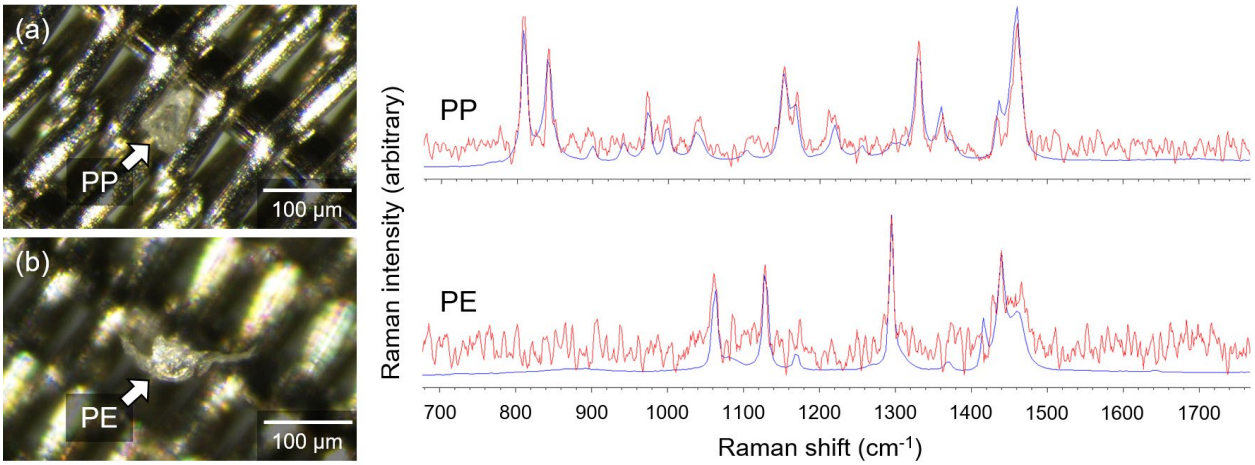

Figure 3.10 Microplastic fragments extracted from (a) *Perna viridis* and (b) *Trachurus japonicus* and retained on stainless-steel filter membranes with a plain Dutch weave pattern. The two fragments were identified to be polypropylene (PP) and polyethylene (PE), respectively, by comparing their Raman spectra (red) to the reference spectra (blue).

3.4 Discussion

3.4.1 Stainless steel as a suitable substrate for Raman analysis

Filter membranes made of glass fibres and cellulose esters are widely used in the extraction of microplastics from biological and food samples (Hermabessiere et al., 2019; Gündoğdu et al., 2020; Sathish et al., 2020). However, these materials are sensitive to Raman excitation that can cause interference to the identification of microplastics. Our findings confirmed a strong fluorescence near 1400 cm^{-1} produced by the glass-fibre filter membranes when excited at 785 nm (Fig. 3.2a; Tuschel, 2016). The use of cellulose-ester filter membranes was associated with weaker fluorescence, but displayed distinct Raman bands in the region of 800–1400 cm^{-1} , which would overlap the characteristic peaks of common plastic polymers and hamper the identification of microplastics (see Fig. 3.7; Castro et al., 2011). This interference appeared to be size-dependent and was significant on 10 µm particles, which were not identifiable when the matching index reduced by up to 100% compared with the 100–300 µm particles (Fig. 3.2b, c).

Apart from glass fibres and cellulose esters, interference to Raman measurements was found to be common among filter membranes made of other materials. One possible solution to this issue is to coat a layer of Raman-insensitive materials such as aluminium on the filter membranes using electron beam evaporation (Oßmann et al., 2017). However, this surface modification process can be time-consuming and requires specific facilities and skilled personnel, requirements that may not be cost-effective for routine monitoring purposes. In this regard, the use of stainless steel can provide a low-cost option with satisfactory performance. In our study, the stainless-steel filter membranes produced minimal fluorescence and Raman excitation (Fig. 3.2a), and the highest matching index among all tested types (Fig. 3.2b, c; Lankers, 2019). It should be noted that the same 10× objective was used to fairly compare the Raman spectra obtained from PS across the size range of 10–300 µm on the three substrate materials. However, within the same laser spot size, a smaller particle is associated with a larger amount of background signal and therefore the Raman matching index is bound to be reduced. This issue can be addressed by using a higher-magnification objective, and that the matching index of 10 µm PS on stainless steel (0.43) can be increased to 0.94 on average under the same configuration but with a 50× objective.

3.4.2 Treatment KHE as an improved method to extract microplastics

This study tested the biomass digestion efficiency of KOH (treatment K) and attempted to improve its performance by adding H_2O_2 (treatment KH), and H_2O_2 with EDTA (treatment KHE; see Table 3.1). In line with earlier studies, treatment K and treatment KH were both effective in digesting organic matter, with almost 100% digestion efficiency achieved for the mussel biomass in terms of dry weight (Fig. 3.3a; Teng et al., 2019; Thiele et al., 2019; Zhang et al., 2020). However, a substantial amount of light-weighed undigested biomass was still observed after the treatments (Fig. 3.3b). The remaining biomass mainly comprised the inorganic content, e.g. in the mussel mantle, and could be associated with autofluorescence that interfered with Raman analysis. As for the fish samples, treatment K and treatment KH were less effective, leaving behind > 20% undigested biomass including the inorganic content in fish bones (Fig. 3.3a). Likewise, in earlier studies, fish bones or inorganic substances that remained in the alimentary tract of fish were not fully digestible in KOH or H_2O_2 (Dehaut et al., 2016; Karami et al., 2017). Apart from the issue of autofluorescence, the relatively large amount of remaining biomass could easily clog the filter membranes and disrupt the extraction process of microplastics (Fig. 3.3b). In this regard, a density separation step could be used to isolate microplastics from the inorganic matter. However, the approach of density separation is less applicable for higher-density microplastics, potentially leading to the loss of these particles which should be avoided (Karami et al., 2017; Lusher et al., 2017).

Treatment KHE containing EDTA was developed to improve the biomass digestion efficiency and bypass the need of density separation. EDTA is a chelating agent used for gentle decalcification and was found useful here in digesting inorganic matter in the biomass, with almost 100% digestion efficiency achieved for both mussel and fish samples (Fig. 3.3a; Bancroft and Gamble, 2008). The amount of undigested biomass was dramatically reduced in treatment KHE, compared with treatment K and treatment KH (Fig. 3.3b). This approach was tested with seven types of microplastics and achieved high recovery rates of 90–100% (Table 3.4). However, slight peeling was observed on some of the particles after treatment KHE, an effect that might be associated with the increased surface area of PP. The surface area was also found to increase in *PVC, which appeared to have formed* crevices and pits after treatment KHE (Fig. 3.5 and 3.6). These changes might be due to the corrosive effect of KOH, but further investigation is needed to confirm our observations (Karami et al. 2017). Nevertheless, the surface modification of PP and PVC was

considered negligible in their identification using Raman spectroscopy, given the very high similarity between the Raman spectra before and after treatment KHE, i.e. 99% and 95%, respectively (Fig. 3.7; Table 3.5). Surface modification was not observed in the other types of microplastics after treatment KHE, whose Raman spectra before and after treatment were 94–99% similar (Fig. 3.7; Table 3.5).

3.4.3 An automated Raman mapping approach to identify microplastics

Treatment KHE was suggested to be an effective approach to extract microplastics from seafood samples. The soft tissue of *P. viridis* and whole fish of *T. japonicus* including bones were used for demonstration, where microplastics were isolated on stainless-steel filter membranes and were identified using a Raman mapping technique (Fig. 3.8). This automated approach represents a great advance from the conventional time-consuming visual assessment and point acquisition approach to assess particles one by one, a method that is prone to handling errors, particularly for particles < 250 µm.

The resolution of Raman spectrometry can theoretically detect microplastics as small as 1–2 µm, while recent research has further improved this size detection limit to 0.1 µm (Sobhani et al., 2019, 2020; Xu et al., 2019; Levermore et al., 2020). However, a higher resolution is associated with a longer analysis time and therefore the areas of interest were usually small in the evaluation of Raman mapping methods (e.g. 88 µm × 88 µm in Sobhani et al. 2019, at 1 µm per pixel). It could be challenging to apply these high-resolution techniques in the environmental or food assessment of microplastics, given the increasing difficulty to isolate smaller-sized particles from the environmental or biological matrices and that the filter membranes could be easily clogged during the microplastic extraction process. In this connection, our goal is to develop a Raman mapping approach that is more suitable for routine monitoring purposes. In the present study, a spatial resolution of 28.4 µm was used to target microplastics > 30 µm. With this resolution, the scanned area was increased to 8,000 µm × 8,000 µm and that the analysis time was controlled to about 14 h, which can be automatically run overnight to maximise productivity. However, certainly there are more advanced Raman or FTIR spectroscopes available in the market which can complete the same area of mapping in a shorter period of time. The actual protocol and analysis time should

therefore be adjusted according to the ease of accessibility to equipment and the target size range of microplastics.

Another concern is that stainless-steel filter membranes, the proposed Raman substrate, usually do not have a homogenous surface (e.g. the plain Dutch weave pattern in Fig. 3.10a), and that the point of focus may not be stable on the target particles during the Raman mapping process. This problem is more pronounced at a higher magnification, but can probably be solved by the auto-focus function available in some Raman spectroscopes. In the present study, a low-magnification (10×) objective was used to address the concern, and the results were found satisfactory for identifying microplastics > 30 µm. With this automated Raman mapping approach, our findings revealed the presence of microplastics in Hong Kong waters, where *P. viridis* contained > 17 times more microplastics than *T. japonicus* per unit wet weight (Fig. 3.9a). This could be attributed to the filter-feeding nature of mussels, which makes them more susceptible than fish to ingestion of suspended particles during the feeding process (Li et al., 2019). Nevertheless, the microplastics determined in *P. viridis* and *T. japonicus* both displayed a similar size range of up to 820 µm and were dominated by PP and PE fragments (Fig. 3.9b and 3.10).

In summary, this study addressed some major technical concerns in microplastic analysis in seafood by developing improved methods for biomass digestion, extraction of microplastics and their characterisation using an automated approach of Raman mapping. Our protocol is applicable to other biological samples and provides an improved alternative to streamline the workflow of microplastic analysis for routine monitoring purposes.

Chapter 4 Microplastics in the edible green-lipped mussel *Perna viridis* in Hong Kong

4.1 Introduction

The global production of plastics has exceeded 359 million tonnes since 2018 and is expected to rise to meet the growing demand (PlasticsEurope, 2019). The increasing use of plastics is often accompanied by plastic pollution, particularly in marine environments. Diverse sorts of plastic waste are becoming pervasive, among which microplastics, i.e. plastic pieces < 5 mm, are posing some of the greatest threats to marine ecosystems (Nava et al., 2020; Wang et al., 2020; Zhang et al., 2021). These small-sized plastics are easily ingested and bioaccumulated, and thus could be transferred to higher-trophic animals along the food chain (Andray, 2011; Jambeck et al., 2015). A lot of these animals serve as seafood for humans, which allows microplastics to enter our diets (Nelms et al., 2018). This is worrying, particularly for Hong Kong, where the seafood consumption per capita can be three times higher than the global average (To and Cheung, 2016).

The sources of microplastics in Hong Kong waters include surface runoff and discharges from sewage treatment plants, along with the riverine input from the Pearl River Estuary (Fok and Cheung, 2015; Mak et al., 2020). It has been confirmed that microplastics are widely found in Hong Kong's coastal and marine environments, including the eastern side where most of the mariculture activities take place (Tsang et al., 2017; Li et al., 2020; Lo et al., 2018, 2020; Wu et al., 2020; Xu et al. 2020a, 2020b). Not surprisingly, microplastics have been found in a number of edible fish species collected from the same areas (Cheung et al. 2018; Chan et al. 2019). Other seafood species are also subject to contamination with microplastics. Among the different types of seafood, bivalve shellfish such as mussels represents a high-risk group of microplastic contamination due to its filter-feeding nature of capturing suspended particles from the water column. For instance, the green-lipped mussel *Perna viridis*, the test species in this study, can filter more than 10 L of seawater and the particles therein per hour per unit g dry weight, a filtration rate which is equivalent to more than 370 L per day per mussel (Tantanasarit et al. 2013). Through consumption of bivalve shellfish, the human ingestion rates of microplastics were estimated to be alarmingly high in some parts of Europe (Van Cauwenberghe and Janssen, 2014; Renzi et al., 2018).

The situation may not be any better in Hong Kong, considering the heavy seafood consumption of its population.

P. viridis is a popular seafood species in the Indo-Pacific region and is widely distributed in Hong Kong waters. This study aimed to quantify and characterise the microplastics in *P. viridis* collected from local mariculture areas, and to estimate the human ingestion rates of microplastics through consumption of *P. viridis*. These rates determined from the Hong Kong population are applicable to other areas in southern China given the similar eating habits and seafood availability in the region. The adoption of an automated mapping technique of Raman microspectroscopy was another highlight of this study. This approach allows the scanning and mapping of microplastics on the whole filter membranes (see Fig. 4.3), offering clear advantages over conventional processes that analyse particles one by one, which are time-consuming and prone to handling errors.

4.2 Materials and Methods

4.2.1 Collection of mussel samples

Mussel sampling was carried out in the mariculture areas of Hong Kong, namely five sites in the northern (N), northeastern (NE), eastern (E) and southeastern waters (SE) and in Tolo Harbour (TH; Fig. 1). The site NE is relatively remote from human activities and would serve as a reference site in this study. The other sites are closer to human settlements or waters contaminated with microplastics (Lo et al., 2018; Mak et al., 2020). In particular, the site TH is located in the vicinity of urbanised areas and is in a land-locked embayment with weak currents, and therefore hypothesised to be the most contaminated site with microplastics (Sin et al., 2003; Lee et al., 2006; Lei et al. 2018). Samples of *P. viridis* with shell lengths of about 80–84 mm (Table 4.1) were handpicked with cotton gloves and stainless-steel scissors at 0.1–2.0 m water depth from the five sites in August–September 2019 (n = 10 per site). Collected samples were transported in cooler bags and stored at –20 ºC in the laboratory until the extraction process of microplastics began.

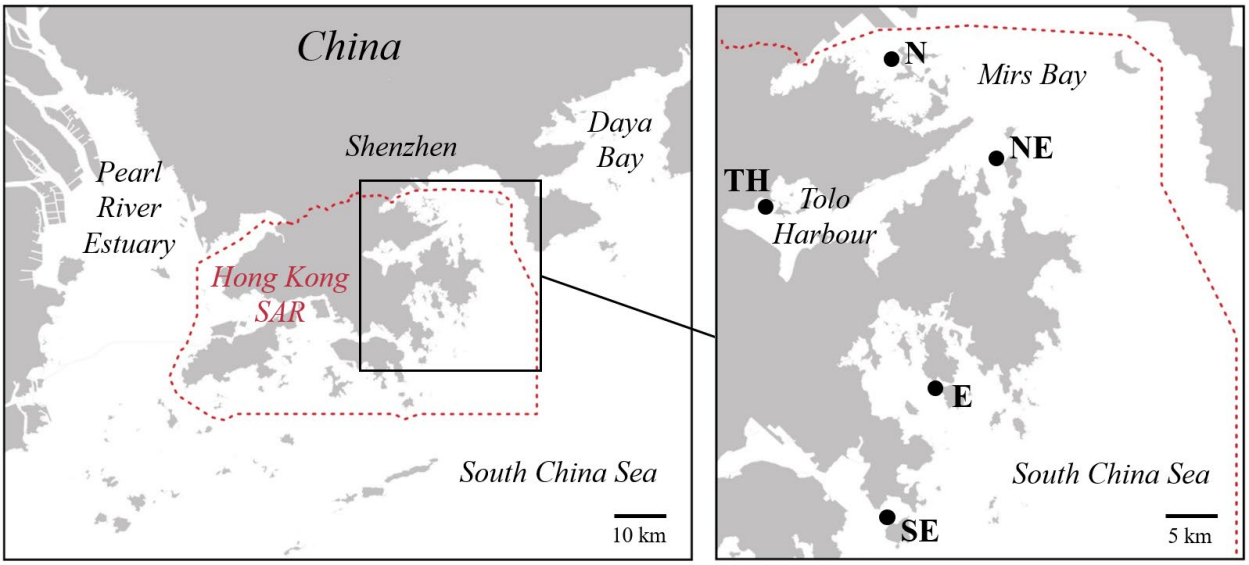

Figure 4.1 Sampling sites of the green-lipped mussel *Perna viridis* in the northern (N), northeastern (NE), eastern (E) and southeastern waters (SE) and in Tolo Harbour (TH), Hong Kong Special Administrative Region (SAR), China. All sites are located within mariculture areas, where the site NE is among the least affected by human activities.

Table 4.1 Biological parameters of the green-lipped mussel *Perna viridis* collected from the five sites in Hong Kong and the number of microplastics in these mussels (mean ± standard deviation; n = 10). Refer to Fig. 4.1 for the site abbreviations and locations. The mussel condition index was estimated as 100 × the ratio of tissue wet weight (g) to shell length (mm). The number of microplastics was standardised per g wet weight or per individual (ind).

Sites	Shell length (mm)	Tissue wet weight (g)	Condition index	Microplastics (items g^{-1})	Microplastics (items ind^{-1})
N	84.4 ± 3.77	9.16 ± 2.23	10.8 ± 2.20	0.23 ± 0.26	2.50 ± 3.60
NE	84.8 ± 2.99	7.93 ± 1.38	9.34 ± 1.53	0.21 ± 0.16	1.60 ± 1.35
TH	83.9 ± 2.57	8.33 ± 1.33	9.91 ± 1.39	1.83 ± 2.52	14.7 ± 19.3
E	80.4 ± 3.94	8.06 ± 1.70	9.99 ± 1.80	0.94 ± 0.49	7.60 ± 4.45
SE	82.7 ± 3.52	10.7 ± 1.80	12.8 ± 1.80	0.54 ± 0.74	5.40 ± 7.17

4.2.2 Extraction of microplastics from mussels

Collected samples of *P. viridis* were thawed at room temperature. Shell length was measured with a digital calliper. Mussel soft tissue was collected with stainless-steel tools, blot-dried on paper towels for wet weight (WW) measurement, and then thoroughly rinsed with Milli-Q water (Merck, Darmstadt, Germany). Microplastics were extracted from the soft tissue of *P. viridis* using the digestion method of Teng et al. (2019), with modification of adding ethylenediaminetetraacetic acid (EDTA), which is commonly used for decalcification in histology and was adopted here to facilitate digestion of the mantle tissue containing calcium carbonate (Bancroft and Gamble, 2008).

In brief, *each rinsed tissue sample was* digested in a 180 mL solution containing 10% potassium hydroxide (KOH) and 14% EDTA at 40 °C for 48 h, during which 10 mL of 30% hydrogen peroxide (H_2O_2) was added twice at 24 h and 42 h to boost the digestion performance. The digestion efficiency of this approach on *P. viridis* biomass was determined to be higher than 99%. Microplastics of of 250–5,000 µm in the solution after digestion were retained on a stainless-steel filter membrane with a pore size of 250 µm using vacuum filtration. The filtrate was furthermore filtered through 30 µm to retrieve microplastics of 30–250 µm.

Several quality assurance measures were implemented during the process of microplastic extraction to minimise contamination. First, all glassware, filtration kits and tools were thoroughly rinsed thrice with Milli-Q water prefiltered by a Merck Millipak 40 Gamma Gold Filter (pore size: 0.22 µm), before each sample analysis. Second, the solutions of 10% KOH, 14% EDTA and 30% H_2O_2 were made with Milli-Q water and filtered through Advantec GC-50 filter membranes (pore size: 0.50 µm; Tokyo, Japan) prior to the tissue digestion treatment. Third, cotton lab coats and nitrile gloves were worn at all times during sample processing. Fourth, the same digestion process was repeated without the mussel samples to serve as the procedural blank (n = 3). Microplastics in the mussel samples and procedural blank, if any, were characterised using Raman microspectroscopy.

4.2.3 Characterisation of microplastics

Microplastics (250–5,000 µm) that were retained on the 250 µm filter membrane were identified using the point acquisition mode of a Renishaw inVia confocal Raman microscope (Wotton-under Edge, UK) equipped with a Leica 10× objective (Wetzlar, Germany) and a 785 nm edge laser (300 mW output power). Raman spectra were acquired for 10 s using 0.1–1% laser power in the wavenumber range of 676–1767 cm^{-1}. Baseline correction, smoothing and cosmic ray removal of the acquired spectra were performed with the Renishaw WiRE 5.2 software. The polymer types of microplastics were identified from these Raman spectra using the Renishaw Polymeric Materials Database. Similarity of each sample spectrum to the reference spectrum was indicated by the matching index provided in WiRE 5.2, which ranged from 0 to 1. A higher value of the index indicated greater similarity, and when > 0.7, the identity of microplastics was accepted. For values of 0.4–0.7, the sample spectra were visually re-examined and were considered microplastics if they contained all characteristic peaks of the reference plastic polymers.

The smaller microplastics (30–250 µm) that were retained on the 30 µm filter membrane was assessed in an automated mapping mode of the Renishaw inVia system using a 785 nm streamline laser. The whole circle that was coated with microplastics (8 mm in diameter) on each filter membrane was scanned at 10% laser power and a spatial resolution of 28.4 µm. Raman spectra were acquired at 5 s per pixel. The mapping process generated more than 10,000 Raman spectra per sample, among which microplastics, if any, were identified using the Renishaw Polymeric Materials Database. Identified microplastics were colour-coded and illustrated in a two-dimensional panel. Other settings and criteria remained the same as in the point acquisition mode.

The shapes and sizes of the identified microplastics were visually verified under a stereomicroscope. Microplastics were categorised into five forms of shape including fragment, fibre, film, rod, and pellet. The size of microplastics in all shapes was expressed as the longest dimension across the area, except for fibre of which the size was measured in length along the central axis. The size measurements were performed on stereomicrographs of the microplastics using the software ImageJ (National Institutes of Health, MD).

4.2.4 Data analysis

The numbers of microplastics in *P. viridis* per unit WW and per individual were compared among the five sites. The data did not fulfil the assumptions of normality or homogeneity of variance, even after data transformation, and were analysed with the Kruskal-Wallis H test (Alam et al., 2019; Lin et al., 2020). If the site effect was significant, Dunn's pairwise comparisons were used to elucidate the spatial pattern of microplastic contamination in the mussels. The significance level was set at 0.05. The statistical procedures were performed with the statistical software SPSS, version 23 (Chicago, IL).

The human ingestion rates of microplastic through mussel consumption were estimated for the Hong Kong population. The calculation was based on the numbers of microplastics determined in *P. viridis* in the present study (on average 0.21–1.83 items g^{-1} WW; Table 4.1), and the consumption rates of bivalve shellfish determined from a local survey in which a total of 5,008 adults participated (see FEHD, 2010). The obtained data in the survey had been age- and gender-weighted to represent a population of 5,394,000 aged 20–84. The mean daily consumption rate was

derived to be 2.29 g person^{-1} d^{-1} for this population, among which 15% had reported to have consumed bivalve shellfish during the survey period, on average at 15.5 g person^{-1} d^{-1} (FEHD, 2010). The two values, 2.29 and 15.5 g person^{-1} d^{-1}, were equivalent to the annual rates of 836 and 5,672 g person^{-1} a^{-1} for the whole population and regular consumers, respectively. These annual rates were used to estimate the lowest end (0.21 × 836 items person^{-1} d^{-1}) and highest end (1.83 × 5,672 items person^{-1} d^{-1}) of the human ingestion rates of microplastics through mussel consumption, and were expressed as items person^{-1} a^{-1}. The rates of microplastic ingestion were also estimated as number per meal, assuming that a portion of 100–250 g WW of mussels was consumed in a meal (Van Cauwenberghe and Janssen, 2014; Renzi et al. 2018; Dowarah et al., 2020; Gündoğdu et al. 2020).

4.3 Results

4.3.1 Spatial comparison of microplastics in mussels

The procedural blank of our method was found to contain 1.33 ± 0.58 items of microplastics (mean ± standard deviation; n = 3). This level of contamination was regarded insignificant and the data obtained from mussels were not corrected. A total of 321 pieces of microplastics were identified in 47 out of 50 mussels collected from the five sites. In these 47 mussels, the abundance of microplastics ranged from 0.08 to 8.60 items g^{-1}, or 1.00 to 66.0 items per individual. The lowest and highest numbers of microplastics in the mussels were detected at the reference site NE and the inner-harbour site TH, respectively. Kruskal-Wallis H test and Dunn's multiple comparisons were used to compare the spatial levels of microplastics in the mussels, which were significantly higher at the sites TH and E than the sites N and NE (Fig. 4.2).

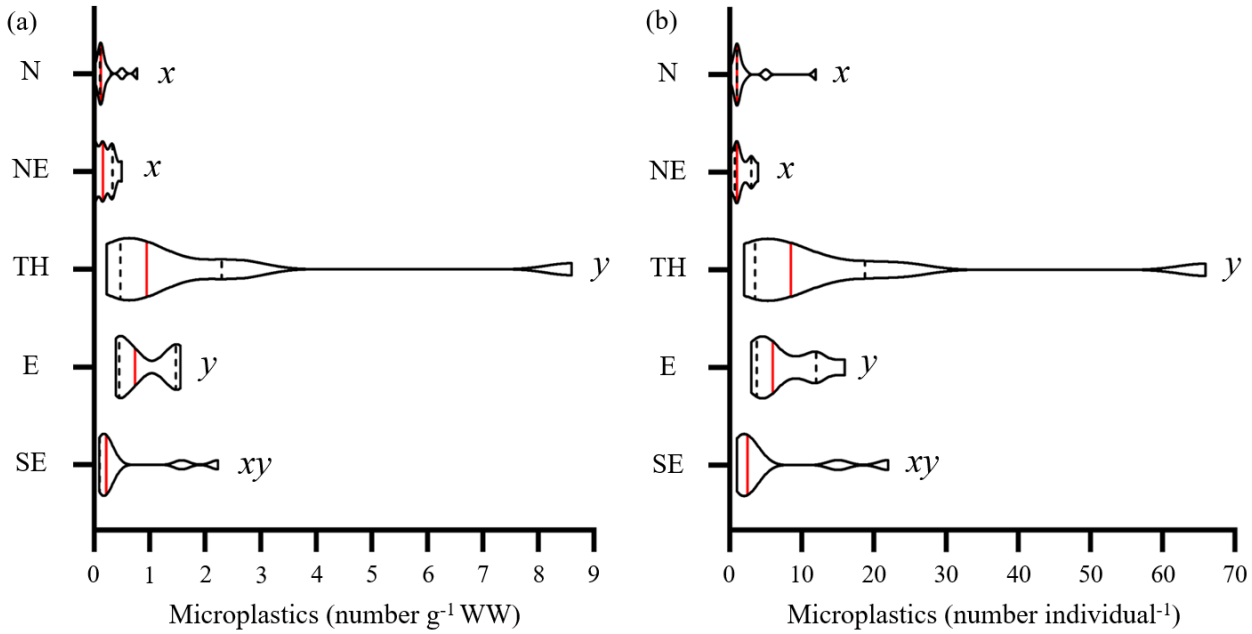

Figure 4.2 Violin plots of the number of microplastics, (a) per g wet weight (WW) and (b) per individual, in the green-lipped mussel *Perna viridis* sampled from the five sites reported in Fig. 4.1 (n = 10). A thicker part of the violin implies a higher frequency of that section of data. The median value is indicated by the red line, while the lower quartile and upper quartile are represented by the dashed black lines. The values of mean and standard deviation among the five sites are reported in Table 4.1. The values at sites indicated with different italic letters (*x*, *y*) were significantly different from each other, as revealed in the Kruskal-Wallis H test for the data (a) per unit WW ($\chi^2(4) = 22.3$, $p < 0.05$) and (b) per individual ($\chi^2(4) = 21.8$, $p < 0.05$), followed by Dunn's multiple comparisons ($p < 0.05$).

4.3.2 Characterisation of microplastics

Microplastics extracted from the mussel samples were assessed using an automated Raman mapping approach (Fig. 4.3). The particle size range of the identified microplastics was 41.7–4,679 µm, but the majority, i.e. 292 pieces out of 321, was smaller than 1,000 µm, while the peak abundance occurred at 90–110 µm (Fig. 4.4). Polypropylene (PP; 56%) was identified to be the most common type of microplastics in total, followed by polyethylene (PE; 25%), polyethylene terephthalate (PET; 10%), and polystyrene (PS; 9.0%). The microplastics mostly existed as fragments (89%) and fibres (9.7%), along with small amounts of films (1.0%) and rods (0.3%). These proportions varied spatially among the five sites (Fig. 4.5a and 4.5b). When the shapes were sorted according to the polymer types, fragments accounted for 93–97% of the numbers of PP, PE and PS microplastics (Fig. 4.6). However, 77% of the PET microplastics were in the form of fibres (Fig. 4.5c).

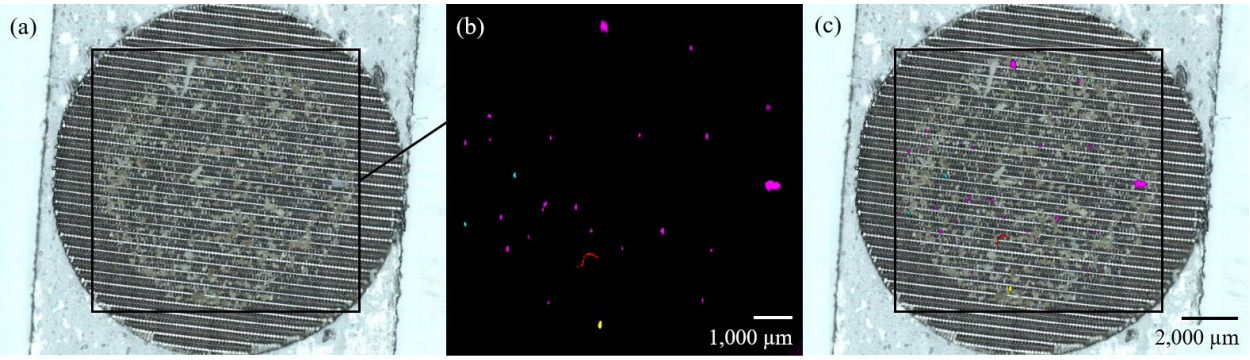

Figure 4.3 (a) Microplastics extracted from *Perna viridis* on a stainless-steel filter membrane (pore size: 31 µm), (b) their colour-coded identification using an automated Raman mapping technique, and (c) the superimposed image of (a) and (b). All particles including microplastics within the black square were scanned and mapped at a spatial resolution of 28.4 µm, from which polypropylene (magenta), polyethylene (cyan), polystyrene (yellow) and polyethylene terephthalate (red) were identified in this example.

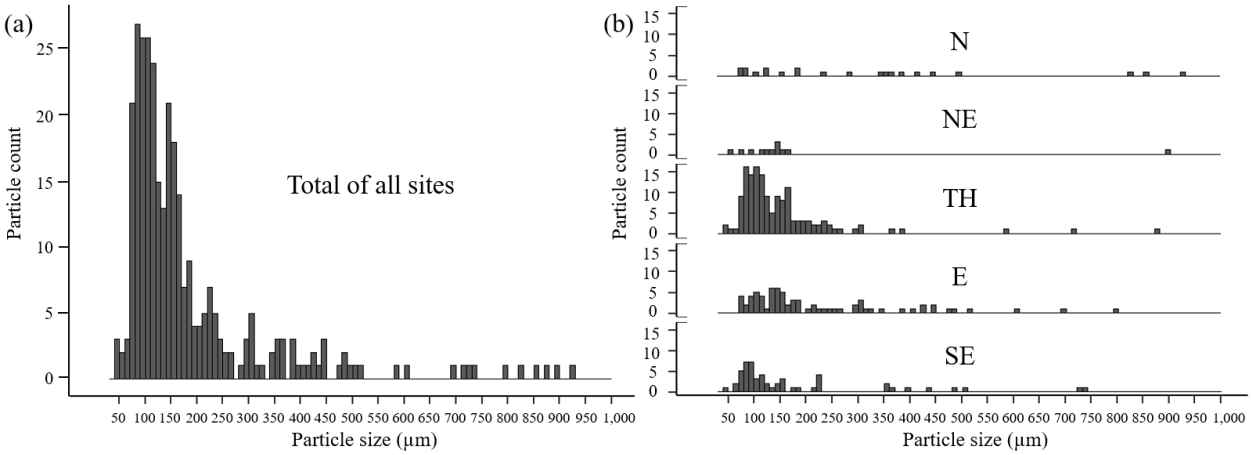

Figure 4.4 Particle size distribution of microplastics extracted from *Perna viridis* (a) across all sampling sites (n = 50) and (b) at each of the five sites (n = 10). The site abbreviations and locations are provided in Fig. 4.1. Microplastics in the size range of 40–1,000 µm accounted for 94% of all microplastics.

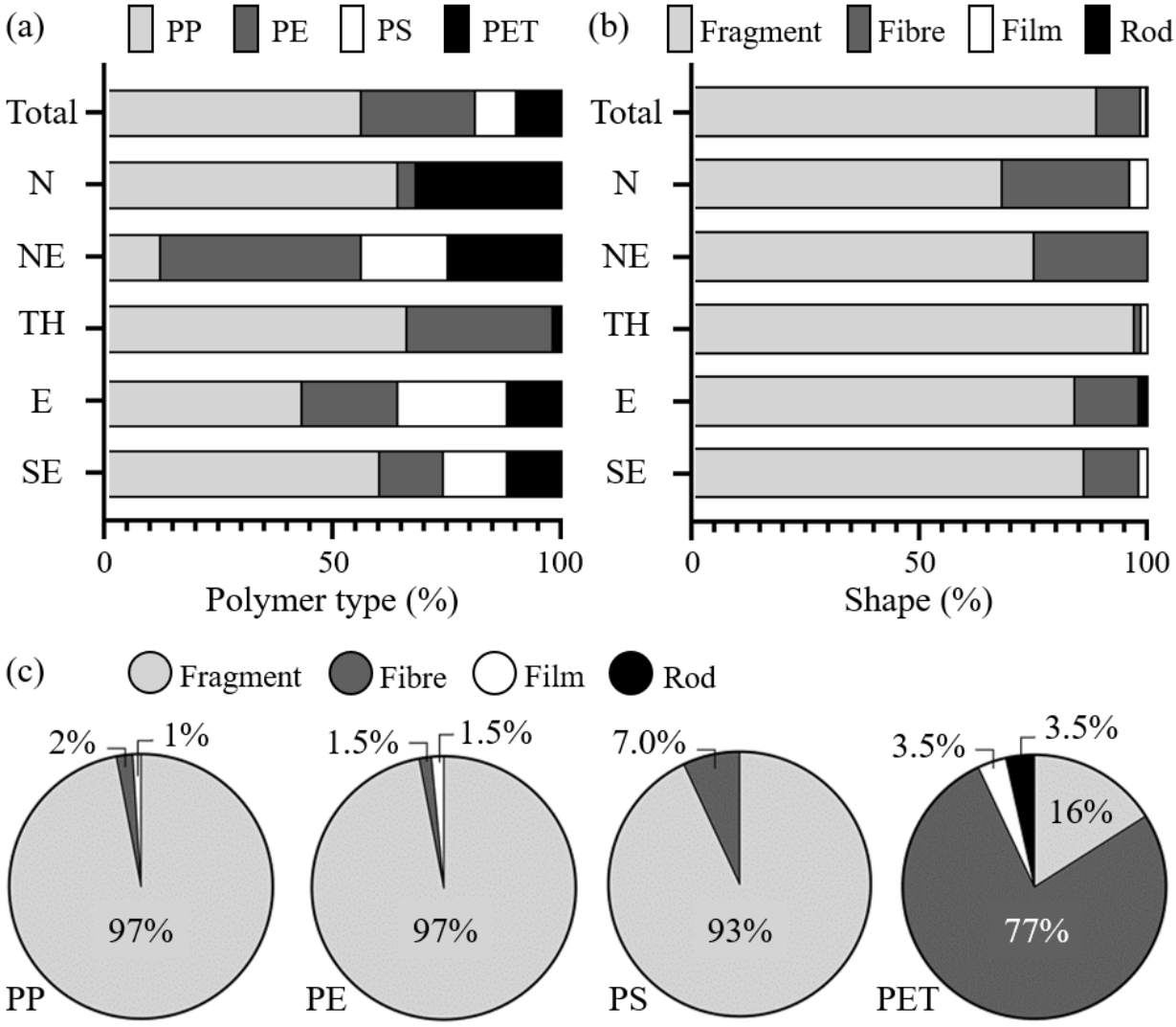

Figure 4.5 The proportions of (a) polymer types, including polypropylene (PP), polyethylene (PE), polystyrene (PS) and polyethylene terephthalate (PET), and (b) shapes of microplastics, including fragment, fibre, film and rod, determined in *Perna viridis* collected from the five sites, and (c) the relative amounts of the four shapes in each polymer type. The pellet shape was not found among the microplastics. Refer to Fig. 4.1 for the abbreviations and locations of the mussel sampling sites.

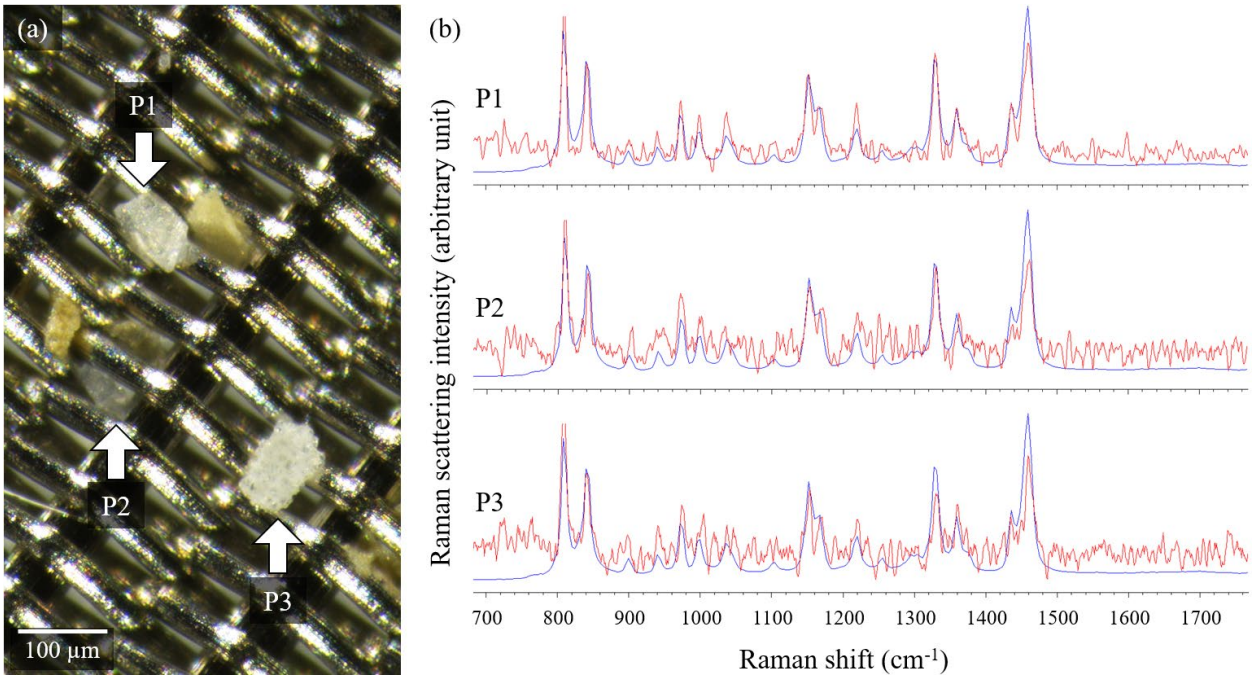

Figure 4.6 (a) Three microplastic fragments extracted from *Perna viridis*, namely P1, P2 and P3, retained on a stainless-steel filter membrane with a plain Dutch weave pattern. (b) The three fragments are identified to be polypropylene by comparing their Raman spectra (red) to the reference spectrum of polypropylene (blue). The two brownish objects are undigested biological materials.

4.3.3 Human ingestion of microplastics through mussel consumption

The lowest and highest mean values of microplastics in *P. viridis* were found to be 0.21 and 1.83 items g^{-1} WW at the sites NE and TH, respectively (Table 4.1). Given the mean consumption rates of bivalve shellfish as 836–5,672 g $person^{-1}$ a^{-1} (FEHD, 2010), the annual human ingestion rates of microplastics through mussel consumption were estimated to be 176–10,380 items $person^{-1}$ a^{-1} in Hong Kong. Moreover, assuming a portion of 100–250 g WW of mussels in a meal, the human ingestion rates of microplastics were calculated to be 21–458 items $meal^{-1}$ (Table 4.2).

Table 4.2 Estimated annual human ingestion rates of microplastics through consumption of bivalve shellfish worldwide. The edible tissue of bivalves was expressed as g wet weight (WW). Different size ranges of microplastics were sampled among studies. Data obtained from the present study are bold.

Species	Sampling area	Mean human consumption rates of bivalves	Mean human ingestion rates of microplastics	Target or detected size range of microplastics	Reference
(a) Rates per year		(g person^{-1} a^{-1})	(items person^{-1} a^{-1})	(μm)	
Magallana gigas	Local market, South Korea	307	21.5	> 43	Cho et al. (2019)
Magallana gigas	Bizerte Lagoon, Tunisia	27.2–3,060	40.3–4,537	> 50	Abidli et al. (2019)
Magallana gigas and *Meretrix lusoria* (and a squid)	Local markets, Taiwan	10,350–14,000	910–1,231	> 20	Chen et al. (2020)
Magallana gigas and *Mytilus edulis*	E coast, France and NW coast, Germany	4,307–26,317	1,800–11,000	> 5.0	Van Cauwenberghe and Janssen (2014)
Mytilus edulis	Local market, South Korea	245	29.4	> 43	Cho et al. (2019)
Mytilus galloprovincialis	W, NW, N and NE coast, Turkey	8,322	1,918	> 70	Gedik and Eryaşar (2020)
Mytilus galloprovincialis	Bizerte Lagoon, Tunisia	31.2–3,510	24.5–2,757	> 50	Abidli et al. (2019)
Mytilus galloprovincialis	Bizerte Lagoon, Tunisia	2.01	4.20	Not reported	Wakkaf et al. (2020)
Mytilus spp. and *Modiolus modiolus*	NW, N and E coast, Scotland	82.0–3,080	123–4,620	> 200	Catarino et al. (2018)
Patinopecten yessoensis	Local market, South Korea	91.3	7.30	> 43	Cho et al. (2019)
Perna viridis	**E coast, Hong Kong**	**836–5,672**	**176–10,380**	**> 30**	**Present study**
Ruditapes decussatus	Bizerte Lagoon, Tunisia	30.4–3,420	43.7–4,920	> 50	Abidli et al. (2019)
Tapes philippinarum	Local market, South Korea	456	155	> 43	Cho et al. (2019)
(b) Rates per meal		(g meal^{-1})	(items meal^{-1})		
Mytilus galloprovincialis	Local markets, Italy	225	1,395–1,620	> 750	Renzi et al. (2018)
Mytilus galloprovincialis (as stuffed mussels)	Local markets, Turkey	100–250	5.80–14.4	Not reported	Gündoğdu et al. (2020)
Perna viridis	**E coast, Hong Kong**	**100–250**	**21–458**	**> 30**	**Present study**
Perna viridis and *Meretrix meretrix*	SE coast, India	121	152	Not reported	Dowarah et al. (2020)

*The human ingestion rate of microplastics divided by the human consumption rate of bivalves

4.4 Discussion

This study investigated the contamination levels of microplastics in *P. viridis* collected from the mariculture areas of Hong Kong. Microplastics extracted from the mussels were counted and characterised using an automated mapping technique of Raman microspectroscopy. Our work revealed higher numbers of microplastics in *P. viridis* at sites closer to human settlement, and that the local human population could ingest up to 10,380 items of microplastics per person per year. These findings highlight the severity of microplastic contamination in seafood and its potential ecological and human health impacts in Hong Kong and adjacent areas.

4.4.1 Spatial comparison of microplastics in mussels

The mean numbers of microplastics in Hong Kong waters were determined to be 51–27,909 items per 100 m^3 (Tsang et al. 2017, 2020; Cheung et al. 2018b). Along the coastline of Hong Kong, microplastics were also found in a diversity of fauna including 42 species of bivalves, barnacles, gastropods and crabs, at up to 9.68 items per g WW or 18.4 items per individual on average (Xu et al. 2020a, 2020b). Likewise, microplastics were detected in *P. viridis* at a similar range of 0.08–8.60 items per g WW or 1.00–66.0 items per individual in this study. The mussels collected from the sites TH and E contained significantly higher numbers of microplastics among the five sites in Hong Kong, both per g WW and per individual (Fig. 4.1 and 4.2; Table 4.1). The greater proximity of the site TH to human settlement that can be associated with plastic pollution possibly led to the more abundant microplastics determined in *P. viridis* (Hantoro et al., 2019). The second highest quantity of microplastics was found at the site E, a popular spot for marine recreational activities such as fishing, kayaking and scuba diving. These human activities could be sources of plastic pollution. Bioaccumulation of xenobiotics in mussels including *P. viridis* has been widely used for pollution monitoring purposes (e.g. Leung et al., 2011; Pinto et al., 2015; Yeung et al., 2017). As for microplastics, recent studies identified a close alignment between the number of microplastics found in mussels and that in the surrounding water, suggesting the applicability of using mussels in the environmental assessment of microplastics (Qu et al., 2018; Li et al., 2019; Wakkaf et al., 2020). In this connection, our findings from *P. viridis* indicated the abundance of microplastics in the mariculture areas of Hong Kong. Other local mariculture species are also subject to microplastic contamination. For instance, microplastics were detected in the flathead grey mullet *Mugil cephalus* collected near the site TH (Cheung et al. 2018a). In their study, PP and PE were the two

most common polymer types identified in the fish, a result that was in line with our findings from *P. viridis* (Fig. 4.5a).

4.4.2 Characterisation of microplastics

The present study applied a Raman mapping technique to count and characterise microplastics, showing clear advantages over the conventional visual sorting step which is prone to observer bias and often associated with high variance in the estimation of particle numbers. Meanwhile, given the increasing difficulty to handpick smaller-sized particles, the common analytical procedure to identify microplastics one by one can be labour intensive and subject to handing errors (GESAMP 2016; Lavers et al., 2016). These concerns were here resolved by the automated mapping approach, in which Raman spectra were acquired from the whole area coated with particles and, from these spectra (> 10,000 spectra on an 8 mm circle), microplastics were identified and colour-coded (Fig. 4.3). This approach allowed the size distribution pattern of microplastics to be elucidated at a higher resolution (Fig. 4.4). The size range of microplastics determined in *P. viridis* was aligned with those from other mussel species, in which the majority were smaller than 200 µm (Digka et al., 2018; Li et al., 2018b; Hermabessiere et al.,2019; Ding et al., 2020; Gedik and Eryaşar, 2020). The uptake and bioaccumulation of microplastics in mussels may be size-dependent. For instance, the Mediterranean mussel *Mytilus galloprovincialis* showed the longest gut retention time for PS particles of 90 µm, but particles of 1–10 µm were rapidly excreted (Kinjo et al., 2019). Another study reported a higher uptake rate on phytoplankton of < 100 µm, compared to 200 µm, by the New Zealand green-lipped mussel *P. canaliculus* (Webb et al., 2019). Likewise, a peak abundance of microplastics at 90–110 µm was determined in *P. viridis* in the present study (Fig. 4.4).

Four polymer types including PP (56%), PE (25%), PS (9.0%) and PET (10%) were identified among the microplastics in the forms of fragment (89%), fibre (9.7%), film (1.0%) and rod (0.3%; Fig. 5a and b). PP, PE and PS are commonly used in food packages, single-use cutlery and carrier bags, among others, which are of disposable nature that often end up in waterways and seas and can be fragmented into microplastics through mechanical and photochemical degradation processes (Andrady, 2011). These PP, PE and PS microplastics are generally positively or neutrally buoyant in nature, suspending in the water column which easily encounter with intertidal animals including *P. viridis*. The fragment form dominated among the PP, PE and PS particles (93–97%;

Fig. 5c). However, only 16% of the PET microplastics occurred as fragments while the majority were confirmed to be fibres (77%; Fig. 5c). Apart from disposable bottle waste, a more significant source of PET microplastics may be the domestic laundry process in which a single garment could shed up to 1,900 fibres per wash (Browne et al., 2011). A lot of these fibres are made of PET that can be released into marine environments via municipal wastewater discharge (Browne et al., 2011; Napper and Thompson, 2016; Jönsson et al., 2018). PET is generally negatively buoyant, but the sinking rates can be influenced by the particle sizes and shapes, among which fibre-shaped microplastics appeared to sink more slowly than other shapes with the same density (Kowalski et al., 2016). The likely longer retention time of PET fibres in surface water provided an explanation for their presence in *P. viridis* sampled in < 2.0 m depth.

4.4.3 Human ingestion of microplastics through mussel consumption

Seafood consumption is known as a significant pathway for microplastics to enter human diets, particularly in the coastal populations that rely on seafood as a primary source of protein. In the case of Hong Kong, our findings indicated that an adult could ingest 21–458 items of microplastics per meal, or 176–10,380 items per year, through consumption of bivalve shellfish including *P. viridis*. These numbers were considered high among the values reported elsewhere (Table 4.2). However, compared to mussel consumption, it has been suggested that the household dust fallout during a meal could lead to an even higher rate of microplastic ingestion (Catarino et al. 2018). Nevertheless, to us the two estimates are not mutually exclusive but additive, as the former determines the amount of microplastics in food ingredients while the latter concerns about the contamination of microplastics in food preparation or in the dining environment.

Another point to be noted is that the predicted values summarised in Table 4.2 represented only rough estimates which relied on assumptions in the calculation, e.g. using an assumed annual consumption rate of bivalves. Nevertheless, these estimates are important in the primary screening to compare microplastic contamination in human diets worldwide and, form these estimates, Hong Kong can be identified as a hotspot of microplastics. There is growing evidence that ingestion of microplastics can cause particle toxicity by inducing immune responses, or chemical toxicity due to leaching of plastic additives or other chemicals (Wright and Kelly, 2017). The chronic human health effects, which are of greater concern in the dietary exposure to microplastics, however

remain largely unclear. Overall, our results from *P. viridis* suggest the abundance of microplastics in the mariculture environment. These findings warrant further investigation on the microplastic contamination in other seafood species and, on a longer term, the human health risk of microplastics through seafood consumption.

Chapter 5 Conclusions and Suggestions for Future Research

5.1 Conclusions

The prevalence of microplastics around the world's oceans has raised serious concerns about their ecological consequences and the potential human health risk of consuming seafood contaminated with microplastics. There have been global research efforts to determine the abundance of microplastics, but the diverse approaches adopted in different studies have made data comparison difficult among regions. Each of these approaches has its own advantages and limitations, and that the common techniques used for extraction and characterisation of microplastics were reviewed in Chapter 2. The literature review focused on marine mussels and fishes, two important groups of seafood worldwide. Major technical challenges were identified from these studies, including the different target size ranges of microplastics, the tendency to underestimate smaller-sized microplastics, the damage on microplastics in various chemical treatments, the potential sample loss due to handling, and the tedious process to assess the plastic particles manually.

These challenges to assess microplastics were addressed in Chapter 3 by developing an improved protocol based on Raman microspectroscopy, using the green-lipped mussel *Perna viridis* and the Japanese jack mackerel *Trachurus japonicus* as the seafood models. Here, we developed a combined chemical treatment that achieved 99–100% biomass digestion efficiency to extract microplastics, with 90–100% recovery rates and negligible Raman interference. The surface damage to microplastics by the use of these chemicals was minimal. The developed treatment was combined with an automated Raman mapping approach to streamline the workflow and to reduce handling errors in the processing of microplastics. With this improved protocol, in Chapter 4 we monitored the amount of microplastics in the mariculture areas of Hong Kong. The monitoring study focused on *P. viridis*, a filter-feeding mussel species commonly used in marine pollution biomonitoring. Our findings identified an inner-harbour site as a local hotspot of microplastics, in which the human ingestion rate of microplastics could go up to 10,380 items of microplastics per person per year through consumption of mussels. These rates are among the highest worldwide, suggesting the potential human health risk of microplastics to the Hong Kong population.

5.2 Suggestions for Future Research

An automated mapping technique of Raman microspectroscopy has been developed in this project to assess microplastics, which can be scanned and located all at once over a particular surface, offering clear advantages over the conventional processes to analyse microplastics on an individual basis. The present study represents a pioneer investigation to adopt this technique for assessing microplastics in seafood samples. Our protocol is applicable to other biological samples that can serve as an improved alternative to streamline the workflow of microplastic analysis for routine monitoring purposes.

Our direction for future research is to lower the particle size detection limit. The target size range of microplastics in the present study has been set to be 31–5,000 μm, a detection level which is not worse than many other studies but can potentially be further extended to particles < 31 μm which were not retained in the existing approach. This proposal appears to be feasible, given that Raman microspectroscopy can theoretically detect microplastics as small as 1 μm. Smaller-sized microplastics, which are more often missed out in the monitoring programmes, could be however more abundant in number than the larger size classes in marine environments, as estimated by Lenz et al. (2016). Moreover, these smaller-sized particles could be biologically more harmful, considering the higher chance to be ingested and enter cells, and therefore should not be excluded in the monitoring programmes.

There are technical issues to be addressed, including the longer analysis time to assess the smaller size range of microplastics. Under the current specifications for microplastics of 31–250 μm, a circular area of 8 mm in diameter was scanned at a spatial resolution of 28.4 μm using a 10× objective at 5 s per pixel to acquire Raman spectra over the whole area. This scanning process required 12–15 h (see Chapter 2). To modify the protocol for microplastics < 31 μm, we have attempted to adjust the spatial resolution to 1.3 μm using a 50× objective. The acquisition time remained at 5 s per pixel. A smaller scanned area at 2 mm in diameter was used to reduce the required time, but it still took more than 700 h to complete the Raman analysis for one sample, which is clearly not practical (Table 5.1). Any further decrease in the scanned area, i.e. the filter membrane area to retain microplastics, is not recommended as it can be easily clogged during the filtration process according to our preliminary findings. Nevertheless, using a less fine resolution

at 4.3 or 14.2 µm may be a good compromise between the size detection limit and analysis time (11 or 33 h; Table 5.1).

Table 5.1 Required analysis time under different specifications of the automated Raman mapping approach for microplastics using a Renishaw inVia confocal Raman microspectrometer (Wotton-under Edge, UK). The present approach for 31–250 µm microplastics is shown in the first row.

Area to be scanned, in diameter	Filter membrane pore size	Objective	Spatial resolution	Acquisition time per spectrum	Analysis time
8 mm	31 µm	10×	28.4 µm	5 s	15 h
5 mm	15 µm	10×	14.2 µm	5 s	11 h
2 mm	5 µm	50×	4.3 µm	5 s	33 h
2 mm	1 µm	50×	1.3 µm	5 s	720 h

Another means to increase the spatial resolution of Raman mapping is switching to a higher-magnification objective, which, however, usually has a narrower depth of view. In other words, a slight change in the surface topology of the scanned area may cause out-of-focus and result in poor Raman signals. This can be a concern for many commonly available filter membranes, which are not perfectly flat on the surface. This issue can be addressed by the auto-focus technology, which is available in some recent models of Raman microscopes but can be expensive. An alternative approach is to use a porous silicon membrane as the Raman substrate, which can be made by electrochemical etching of a silicon wafer and is flat on the top surface. In our preliminary study, polystyrene particles of > 1 µm can be identified on the silicon membrane (0.8 µm pore size) using a 100× objective and the same Raman mapping approach, but further optimisation is required to extend the application to other types of smaller-sized microplastics. Overall, the findings presented in this thesis provide a solid foundation for future research on assessing microplastics in seafood and other biological samples.

References

Abidli, S., Lahbib, Y., & El Menif, N. T. (2019). Microplastics in commercial molluscs from the lagoon of Bizerte (Northern Tunisia). *Marine Pollution Bulletin* 142, 243-252.

Akhbarizadeh, R., Moore, F., & Keshavarzi, B. (2018). Investigating a probable relationship between microplastics and potentially toxic elements in fish muscles from northeast of Persian Gulf. *Environmental Pollution* 232, 154-163.

Alam, F. C., Sembiring, E., Muntalif, B. S., & Suendo, V. (2019). Microplastic distribution in surface water and sediment river around slum and industrial area (case study: Ciwalengke River, Majalaya district, Indonesia). *Chemosphere* 224, 637-645.

Al-Lihaibi, S., Al-Mehmadi, A., Alarif, W. M., Bawakid, N. O., Kallenborn, R., & Ali, A. M. (2019). Microplastics in sediments and fish from the Red Sea coast at Jeddah (Saudi Arabia). *Environ Chem* 16, 641-650.

Alomar, C., Sanz-Martín, M., Compa, M., Rios-Fuster, B., Álvarez, E., Ripolles, V., Valencia, J. M. & Deudero, S. (2021). Microplastic ingestion in reared aquaculture fish: Biological responses to low-density polyethylene controlled diets in *Sparus aurata*. *Environmental Pollution* 280, 116960.

Andrady, A. L. (2011). Microplastics in the marine environment. *Marine Pollution Bulletin* 62, 1596-1605.

Arthur, C., Baker, J., & Bamford, H. (2009). International research workshop on the occurrence, effects, and fate of microplastic marine debris. In *Conference Proceedings. Sept* (pp. 9-11).

Avio, C. G., Gorbi, S., & Regoli, F. (2015). Experimental development of a new protocol for extraction and characterization of microplastics in fish tissues: First observations in commercial species from Adriatic Sea. *Marine Environmental Research* 111, 18-26.

Bagheri, T., Gholizadeh, M., Abarghouei, S., Zakeri, M., Hedayati, A., Rabaniha, M., Aghaeimoghadam, A., & Hafezieh, M. (2020). Microplastics distribution, abundance and composition in sediment, fishes and benthic organisms of the Gorgan Bay, Caspian sea. *Chemosphere*, 127201.

Bancroft, J. D., & Gamble, M. (Eds.). (2008). *Theory and practice of histological techniques*. Elsevier health sciences.

Batel, A., Linti, F., Scherer, M., Erdinger, L., & Braunbeck, T. (2016). Transfer of benzo [a] pyrene from microplastics to *Artemia nauplii* and further to zebrafish via a trophic food web experiment: CYP1A induction and visual tracking of persistent organic pollutants. *Environmental Toxicology and Chemistry* 35, 1656-1666.

Bergmann, M., Mützel, S., Primpke, S., Tekman, M. B., Trachsel, J., & Gerdts, G. (2019). White and wonderful? Microplastics prevail in snow from the Alps to the Arctic. *Science Advances* 5, eaax1157.

Beyer, J., Green, N. W., Brooks, S., Allan, I. J., Ruus, A., Gomes, T., Bråte, I. L. N., & Schøyen, M. (2017). Blue mussels (*Mytilus edulis* spp.) as sentinel organisms in coastal pollution monitoring: a review. *Marine Environmental Research* 130, 338-365.

Bianchi, J., Valente, T., Scacco, U., Cimmaruta, R., Sbrana, A., Silvestri, C., & Matiddi, M. (2020). Food preference determines the best suitable digestion protocol for analysing microplastic ingestion by fish. *Marine Pollution Bulletin* 154, 111050.

Birnstiel, S., Soares-Gomes, A., & da Gama, B. A. (2019). Depuration reduces microplastic content in wild and farmed mussels. *Marine Pollution Bulletin* 140, 241-247.

Bishop, G., Styles, D., & Lens, P. N. (2020). Recycling of European plastic is a pathway for plastic debris in the ocean. *Environment International* 142, 105893.

Bonello, G., Varrella, P., & Pane, L. (2018). First evaluation of microplastic content in benthic filter-feeders of the Gulf of La Spezia (Ligurian Sea). *Journal of Aquatic Food Product Technology* 27, 284-291.

Bråte, I. L. N., Hurley, R., Iversen, K., Beyer, J., Thomas, K. V., Steindal, C. C., Green, N. W., Olsen, M., & Lusher, A. (2018). *Mytilus* spp. as sentinels for monitoring microplastic pollution in Norwegian coastal waters: A qualitative and quantitative study. *Environmental Pollution* 243, 383-393.

Browne, M. A., Crump, P., Niven, S. J., Teuten, E., Tonkin, A., Galloway, T., & Thompson, R. (2011). Accumulation of microplastic on shorelines worldwide: sources and sinks. *Environmental Science & Technology* 45, 9175-9179.

Browne, M. A., Dissanayake, A., Galloway, T. S., Lowe, D. M., & Thompson, R. C. (2008). Ingested microscopic plastic translocates to the circulatory system of the mussel, *Mytilus edulis* (L.). *Environmental Science & Technology* 42, 5026-5031.

Castro, K., de Vallejuelo, S. F. O., Astondoa, I., Goñi, F. M., & Madariaga, J. M. (2011). Analysis of confiscated fireworks using Raman spectroscopy assisted with SEM-EDS and FTIR. *Journal of Raman Spectroscopy* 42, 2000-2005.

Catarino, A. I., Macchia, V., Sanderson, W. G., Thompson, R. C., & Henry, T. B. (2018). Low levels of microplastics (MP) in wild mussels indicate that MP ingestion by humans is minimal compared to exposure via household fibres fallout during a meal. *Environmental Pollution* 237, 675-684.

Chagnon, C., Thiel, M., Antunes, J., Ferreira, J. L., Sobral, P., & Ory, N. C. (2018). Plastic ingestion and trophic transfer between Easter Island flying fish (C*heilopogon rapanouiensis*) and yellowfin tuna (*Thunnus albacares*) from Rapa Nui (Easter Island). *Environmental Pollution* 243, 127-133.

Chan, H. S. H., Dingle, C., & Not, C. (2019). Evidence for non-selective ingestion of microplastic in demersal fish. *Marine pollution bulletin* 149, 110523.

Chen, J. Y. S., Lee, Y. C., & Walther, B. A. (2020). Microplastic Contamination of three commonly consumed seafood species from Taiwan: A pilot study. *Sustainability* 12, 9543.

Cheung, L. T., Lui, C. Y., & Fok, L. (2018). Microplastic contamination of wild and captive flathead grey mullet (*Mugil cephalus*). *International Journal of Environmental Research and Public Health* 15, 597.

Cho, Y., Shim, W. J., Jang, M., Han, G. M., & Hong, S. H. (2019). Abundance and characteristics of microplastics in market bivalves from South Korea. E*nvironmental Pollution* 245, 1107-1116.

Claessens, M., Van Cauwenberghe, L., Vandegehuchte, M. B., & Janssen, C. R. (2013). New techniques for the detection of microplastics in sediments and field collected organisms. *Marine Pollution Bulletin* 70, 227-233.

Cole, M., Lindeque, P., Halsband, C., & Galloway, T.S., (2011). Microplastics as contaminants in the marine environment: a review. *Marine Pollution Bulletin* 62*,* 2588–2597.

Cole, M., Webb, H., Lindeque, P. K., Fileman, E. S., Halsband, C., & Galloway, T. S. (2014). Isolation of microplastics in biota-rich seawater samples and marine organisms. *Scientific Reports* 4, 4528.

Collard, F., Gilbert, B., Compère, P., Eppe, G., Das, K., Jauniaux, T., & Parmentier, E. (2017). Microplastics in livers of European anchovies (*Engraulis encrasicolus*, L.). *Environmental Pollution* 229, 1000-1005.

Collicutt, B., Juanes, F., & Dudas, S. E. (2019). Microplastics in juvenile Chinook salmon and their nearshore environments on the east coast of Vancouver Island. *Environmental Pollution* 244, 135-142.

Courtene-Jones, W., Quinn, B., Murphy, F., Gary, S. F., & Narayanaswamy, B. E. (2017). Optimisation of enzymatic digestion and validation of specimen preservation methods for the analysis of ingested microplastics. *Analytical Methods* 9, 1437-1445.

Cozzolino, L., de los Santos, C. B., Zardi, G. I., Repetto, L., & Nicastro, K. R. (2021). Microplastics in commercial bivalves harvested from intertidal seagrasses and sandbanks in the Ria Formosa lagoon, Portugal. *Marine and Freshwater Research*, https://doi.org/10.1071/MF20202.

da Costa, J. P., Santos, P. S., Duarte, A. C., & Rocha-Santos, T. (2016). (Nano) plastics in the environment–sources, fates and effects. *Science of the Total Environment* 566, 15-26.

Daniel, D. B., Ashraf, P. M., & Thomas, S. N. (2020a). Abundance, characteristics and seasonal variation of microplastics in Indian white shrimps (*Fenneropenaeus indicus*) from coastal waters off Cochin, Kerala, India. *Science of the Total Environment* 737, 139839. 15-26.

Daniel, D. B., Ashraf, P. M., & Thomas, S. N. (2020b). Microplastics in the edible and inedible tissues of pelagic fishes sold for human consumption in Kerala, India. *Environmental Pollution* 266, 115365.

De Sá, L. C., Luís, L. G., & Guilhermino, L. (2015). Effects of microplastics on juveniles of the common goby (*Pomatoschistus microps*): Confusion with prey, reduction of the predatory performance and efficiency, and possible influence of developmental conditions. *Environmental Pollution* 196, 359-362.

De Sá, L. C., Oliveira, M., Ribeiro, F., Rocha, T. L., & Futter, M. N. (2018). Studies of the effects of microplastics on aquatic organisms: what do we know and where should we focus our efforts in the future? *Science of the Total Environment* 645, 1029-1039.

De Witte, B., Devriese, L., Bekaert, K., Hoffman, S., Vandermeersch, G., Cooreman, K., & Robbens, J. (2014). Quality assessment of the blue mussel (*Mytilus edulis*): Comparison between commercial and wild types. *Marine Pollution Bulletin* 85, 146-155.

Dehaut, A., Cassone, A. L., Frère, L., Hermabessiere, L., Himber, C., Rinnert, E., Rivière, G., Lambert, C., Soudant, P., Huvet, A., Duflos, G., & Paul-Pont, I. (2016). Microplastics in seafood: Benchmark protocol for their extraction and characterization. *Environmental Pollution* 215, 223-233.

Derraik, J. G. (2002). The pollution of the marine environment by plastic debris: a review. *Marine Pollution Bulletin* 44, 842-852.

Digka, N., Tsangaris, C., Kaberi, H., Adamopoulou, A., & Zeri, C. (2018a). Microplastic abundance and polymer types in a Mediterranean environment. In *Proceedings of the International Conference on Microplastic Pollution in the Mediterranean Sea* (pp. 17-24). Springer, Cham.

Digka, N., Tsangaris, C., Torre, M., Anastasopoulou, A., & Zeri, C. (2018b). Microplastics in mussels and fish from the Northern Ionian Sea. *Marine Pollution Bulletin* 135, 30-40.

Ding, J., Li, J., Sun, C., Jiang, F., He, C., Zhang, M., Ju, P., & Ding, N. X. (2020). An examination of the occurrence and potential risks of microplastics across various shellfish. *Science of the Total Environment* 739, 139887.

Ding, J. F., Li, J. X., Sun, C. J., He, C. F., Jiang, F. H., Gao, F. L., & Zheng, L. (2018). Separation and identification of microplastics in digestive system of bivalves. *Chinese Journal of Analytical Chemistry* 46, 690-697.

Directive, S. F., 2013. *Guidance on monitoring of marine litter in European Seas*. European Commission, 125 pp.

Dowarah, K., Patchaiyappan, A., Thirunavukkarasu, C., Jayakumar, S., & Devipriya, S. P. (2020). Quantification of microplastics using Nile Red in two bivalve species *Perna viridis* and *Meretrix meretrix* from three estuaries in Pondicherry, India and microplastic uptake by local communities through bivalve diet. *Marine Pollution Bulletin* 153, 110982.

EFSA Panel on Contaminants in the Food Chain (CONTAM). (2016). Presence of microplastics and nanoplastics in food, with particular focus on seafood. *EFSA Journal* 14, e04501.

Fang, C., Zheng, R., Chen, H., Hong, F., Lin, L., Lin, H., Guo, H., Bailey, C., Segner, H., Mu, J., & Bo, J. (2019). Comparison of microplastic contamination in fish and bivalves from two major cities in Fujian province, China and the implications for human health. *Aquaculture* 512, 734322.

FEHD (2010). *Hong Kong Population Based Food Consumption Survey 2005-2007*, Food and Environmental Hygiene Department (FEHD), Hong Kong, 60 pp.

Feng, Z., Zhang, T., Li, Y., He, X., Wang, R., Xu, J., & Gao, G. (2019). The accumulation of microplastics in fish from an important fish farm and mariculture area, Haizhou Bay, China. *Science of the Total Environment* 696, 133948.

Filgueiras, A. V., Preciado, I., Cartón, A., & Gago, J. (2020). Microplastic ingestion by pelagic and benthic fish and diet composition: A case study in the NW Iberian shelf. *Marine Pollution Bulletin* 160, 111623.

Fok, L., & Cheung, P. K. (2015). Hong Kong at the Pearl River Estuary: A hotspot of microplastic pollution. *Marine Pollution Bulletin* 99, 112-118.

Fortelný, I., Michálková, D., & Kruliš, Z. (2004). An efficient method of material recycling of municipal plastic waste. *Polymer Degradation and Stability* 85, 975-979.

Frias, J. P. G. L., & Nash, R. (2019). Microplastics: finding a consensus on the definition. *Marine Pollution Bulletin* 138, 145-147.

Garcia-Garin, O., Vighi, M., Aguilar, A., Tsangaris, C., Digka, N., Kaberi, H., & Borrell, A. (2019). *Boops boops* as a bioindicator of microplastic pollution along the Spanish Catalan coast. *Marine Pollution Bulletin* 149, 110648.

Garnier, Y., Jacob, H., Guerra, A. S., Bertucci, F., & Lecchini, D. (2019). Evaluation of microplastic ingestion by tropical fish from Moorea Island, French Polynesia. *Marine Pollution Bulletin* 140, 165-170.

Gedik, K., & Eryaşar, A. R. (2020). Microplastic pollution profile of Mediterranean mussels (*Mytilus galloprovincialis*) collected along the Turkish coasts. *Chemosphere* 260, 127570.

GESAMP (2016) *Sources, fate and effects of microplastics in the marine environment: part two of a global assessment*, Reports and Studies 93, Joint group of experts on the scientific aspects of marine environmental protection (GESAMP), London, 220 pp.

Giani, D., Baini, M., Galli, M., Casini, S., & Fossi, M. C. (2019). Microplastics occurrence in edible fish species (*Mullus barbatus* and *Merluccius merluccius*) collected in three different geographical sub-areas of the Mediterranean Sea. *Marine Pollution Bulletin* 140, 129-137.

Gomiero, A., Strafella, P., Øysæd, K. B., & Fabi, G. (2019). First occurrence and composition assessment of microplastics in native mussels collected from coastal and offshore areas of the

northern and central Adriatic Sea. *Environmental Science and Pollution Research* 26, 24407-24416.

Gündoğdu, S., Çevik, C., & Ataş, N. T. (2020). Stuffed with microplastics: microplastic occurrence in traditional stuffed mussels sold in the Turkish market. *Food Bioscience* 37, 100715.

Guzzetti, E., Sureda, A., Tejada, S., & Faggio, C. (2018). Microplastic in marine organism: Environmental and toxicological effects. *Environmental Toxicology and Pharmacology* 64, 164-171.

Halstead, J. E., Smith, J. A., Carter, E. A., Lay, P. A., & Johnston, E. L. (2018). Assessment tools for microplastics and natural fibres ingested by fish in an urbanised estuary. *Environmental Pollution* 234, 552-561.

Hantoro, I., Löhr, A. J., Van Belleghem, F. G., Widianarko, B., & Ragas, A. M. (2019). Microplastics in coastal areas and seafood: implications for food safety. *Food Additives & Contaminants: Part A* 36, 674-711.

Hendrickson, E., Minor, E. C., & Schreiner, K. (2018). Microplastic abundance and composition in western Lake Superior as determined via microscopy, Pyr-GC/MS, and FTIR. *Environmental Science & Technology* 52, 1787-1796.

Hermabessiere, L., Paul-Pont, I., Cassone, A. L., Himber, C., Receveur, J., Jezequel, R., Rakwe, M., Rinnert, E., Rivière, G., Lambert, C., Huvet, A., Dehaut, A., Duflos, G., & Soudant, A. (2019). Microplastic contamination and pollutant levels in mussels and cockles collected along the channel coasts. *Environmental Pollution* 250, 807-819.

Herrera, A., Ŝtindlová, A., Martínez, I., Rapp, J., Romero-Kutzner, V., Samper, M. D., Montoto, T., Aguiar-González, B., Packard, T., & Gómez, M. (2019). Microplastic ingestion by Atlantic chub mackerel (*Scomber colias*) in the Canary Islands coast. *Marine Pollution Bulletin* 139, 127-135.

Hossain, M. S., Rahman, M. S., Uddin, M. N., Sharifuzzaman, S. M., Chowdhury, S. R., Sarker, S., & Chowdhury, M. S. N. (2020). Microplastic contamination in Penaeid shrimp from the Northern Bay of Bengal. *Chemosphere* 238, 124688.

Hossain, M. S., Sobhan, F., Uddin, M. N., Sharifuzzaman, S. M., Chowdhury, S. R., Sarker, S., & Chowdhury, M. S. N. (2019). Microplastics in fishes from the Northern Bay of Bengal. *Science of the Total Environment* 690, 821-830.

Hurley, R. R., Lusher, A. L., Olsen, M., & Nizzetto, L. (2018). Validation of a method for extracting microplastics from complex, organic-rich, environmental matrices. *Environmental Science & Technology* 52, 7409-7417.

Jahan, S., Strezov, V., Weldekidan, H., Kumar, R., Kan, T., Sarkodie, S. A., He, J., Dastjerdi, B., & Wilson, S. P. (2019). Interrelationship of microplastic pollution in sediments and oysters in a seaport environment of the eastern coast of Australia. *Science of the Total Environment* 695, 133924.

Jambeck, J. R., Geyer, R., Wilcox, C., Siegler, T. R., Perryman, M., Andrady, A., Narayan, R., & Law, K. L. (2015). Plastic waste inputs from land into the ocean. *Science* 347, 768-771.

James, K., Vasant, K., Padua, S., Gopinath, V., Abilash, K. S., Jeyabaskaran, R., Babu, A., & John, S. (2020). An assessment of microplastics in the ecosystem and selected commercially important fishes off Kochi, south eastern Arabian Sea, India. *Marine Pollution Bulletin* 154, 111027.

Jemec, A., Horvat, P., Kunej, U., Bele, M., & Kržan, A. (2016). Uptake and effects of microplastic textile fibers on freshwater crustacean *Daphnia magna*. *Environmental Pollution* 219, 201-209.

Jönsson, C., Levenstam Arturin, O., Hanning, A. C., Landin, R., Holmström, E., & Roos, S. (2018). Microplastics shedding from textiles—developing analytical method for measurement of shed material representing release during domestic washing. *Sustainability* 10, 2457.

Jovanović, B. (2017). Ingestion of microplastics by fish and its potential consequences from a physical perspective. *Integrated Environmental Assessment and Management* 13, 510-515.

Käppler, A., Fischer, D., Oberbeckmann, S., Schernewski, G., Labrenz, M., Eichhorn, K. J., & Voit, B. (2016). Analysis of environmental microplastics by vibrational microspectroscopy: FTIR, Raman or both?. *Analytical and Bioanalytical Chemistry* 408, 8377-8391.

Käppler, A., Windrich, F., Löder, M. G., Malanin, M., Fischer, D., Labrenz, M., ... & Voit, B. (2015). Identification of microplastics by FTIR and Raman microscopy: a novel silicon filter substrate opens the important spectral range below 1300 cm− 1 for FTIR transmission measurements. *Analytical and Bioanalytical Chemistry* 407, 6791-6801.

Karami, A., Golieskardi, A., Choo, C. K., Romano, N., Ho, Y. B., & Salamatinia, B. (2017). A high-performance protocol for extraction of microplastics in fish. *Science of the Total Environment* 578, 485-494.

Karbalaei, S., Golieskardi, A., Hamzah, H. B., Abdulwahid, S., Hanachi, P., Walker, T. R., & Karami, A. (2019). Abundance and characteristics of microplastics in commercial marine fish from Malaysia. *Marine Pollution Bulletin* 148, 5-15.

Katija, K., Choy, C. A., Sherlock, R. E., Sherman, A. D., & Robison, B. H. (2017). From the surface to the seafloor: How giant larvaceans transport microplastics into the deep sea. *Science Advances* 3, e1700715.

Kazour, M., Jemaa, S., Issa, C., Khalaf, G., & Amara, R. (2019). Microplastics pollution along the Lebanese coast (Eastern Mediterranean Basin): Occurrence in surface water, sediments and biota samples. *Science of the Total Environment* 696, 133933.

Kim, S. M., Kim, H., Lee, W. C., Kim, H. C., Lee, H., Kwak, S. N., Jo, N., & Lee, S. H. (2016). Monthly variation in the proximate composition of jack mackerel (*Trachurus japonicus*) from Geumo Island, Korea. *Fisheries Research* 183, 371-378.

Kinjo, A., Mizukawa, K., Takada, H., & Inoue, K. (2019). Size-dependent elimination of ingested microplastics in the Mediterranean mussel *Mytilus galloprovincialis*. *Marine Pollution Bulletin* 149, 110512.

Klein, S., Dimzon, I. K., Eubeler, J., & Knepper, T. P. (2018). Analysis, occurrence, and degradation of microplastics in the aqueous environment. In *Freshwater Microplastics* (pp. 51-67). Springer, Cham.

Kolandhasamy, P., Su, L., Li, J., Qu, X., Jabeen, K., & Shi, H. (2018). Adherence of microplastics to soft tissue of mussels: a novel way to uptake microplastics beyond ingestion. *Science of The Total Environment* 610, 635-640.

Kowalski, N., Reichardt, A. M., & Waniek, J. J. (2016). Sinking rates of microplastics and potential implications of their alteration by physical, biological, and chemical factors. *Marine Pollution Bulletin* 109, 310-319.

Laist, D. W. (1987). Overview of the biological effects of lost and discarded plastic debris in the marine environment. *Marine Pollution Bulletin* 18, 319-326.

Laist, D. W. (1997). Impacts of marine debris: entanglement of marine life in marine debris including a comprehensive list of species with entanglement and ingestion records. In *Marine Debris* (pp. 99-139). Springer, New York, NY.

Lankers, M. (2019). Applications in: Environmental analytics (fine particles). *Physical Sciences Reviews* 4.

Lavers, J. L., Oppel, S., & Bond, A. L. (2016). Factors influencing the detection of beach plastic debris. *Marine Environmental Research* 119, 245-251.

Lee, J. H., Harrison, P. J., Kuang, C., & Yin, K. (2006). Eutrophication dynamics in Hong Kong coastal waters: physical and biological interactions. In: Wolanski, E. (Ed.), *The Environment in Asia Pacific Harbours*. Springer, Dordrecht, pp. 187-206.

Lefebvre, C., Saraux, C., Heitz, O., Nowaczyk, A., & Bonnet, D. (2019). Microplastics FTIR characterisation and distribution in the water column and digestive tracts of small pelagic fish in the Gulf of Lions. *Marine Pollution Bulletin* 142, 510-519.

Lei, Y., Whyte, C., Davidson, K., Tett, P., & Yin, K. (2018). A change in phytoplankton community index with water quality improvement in Tolo Harbour, Hong Kong. *Marine Pollution Bulletin* 127, 823-830.

Lenz, R., Enders, K., & Nielsen, T.G. (2016). Microplastic exposure studies should be environmentally realistic. *Proceedings of the National Academy of Sciences of the United States of America* 113, E4121-E4122.

Lenz, R., Enders, K., Stedmon, C. A., Mackenzie, D. M. A., & Nielsen, T. G. (2015). A critical assessment of visual identification of marine microplastic using Raman spectroscopy for analysis improvement. *Marine Pollution Bulletin* 100, 82–91.

Levermore, J. M., Smith, T. E., Kelly, F. J., & Wright, S. L. (2020). Detection of microplastics in ambient particulate matter using Raman spectral imaging and chemometric analysis. *Analytical Chemistry* 92, 8732-8740.

Leung, P. T., Wang, Y., Mak, S. S., Ng, W. C., & Leung, K. M. (2011). Differential proteomic responses in hepatopancreas and adductor muscles of the green-lipped mussel *Perna viridis* to stresses induced by cadmium and hydrogen peroxide. *Aquatic Toxicology* 105, 49-61.

Li, H. X., Ma, L. S., Lin, L., Ni, Z. X., Xu, X. R., Shi, H. H., Yan, Y., Zheng, G. M. & Rittschof, D. (2018a). Microplastics in oysters *Saccostrea cucullata* along the Pearl River estuary, China. *Environmental Pollution* 236, 619-625.

Li, J., Green, C., Reynolds, A., Shi, H., & Rotchell, J. M. (2018b). Microplastics in mussels sampled from coastal waters and supermarkets in the United Kingdom. *Environmental Pollution* 241, 35-44.

Li, J., Lusher, A. L., Rotchell, J. M., Deudero, S., Turra, A., Bråte, I. L. N., Sun, C., Hossain, M. S., Li, Q., Kolandhasamy, P., & Shi, H. (2019). Using mussel as a global bioindicator of coastal microplastic pollution. *Environmental Pollution* 244, 522-533.

Li, J., Qu, X., Su, L., Zhang, W., Yang, D., Kolandhasamy, P., Li, D., & Shi, H. (2016b). Microplastics in mussels along the coastal waters of China. *Environmental Pollution* 214, 177-184.

Li, W. C., Tse, H. F., & Fok, L. (2016a). Plastic waste in the marine environment: a review of sources, occurrence and effects. *Science of the Total Environment* 566-567, 333-349.

Li, W., Lo, H. S., Wong, H. M., Zhou, M., Wong, C. Y., Tam, N. F. Y., & Cheung, S. G. (2020). Heavy metals contamination of sedimentary microplastics in Hong Kong. *Marine Pollution Bulletin* 153, 110977.

Liboiron, F., Ammendolia, J., Saturno, J., Melvin, J., Zahara, A., Richárd, N., & Liboiron, M. (2018). A zero percent plastic ingestion rate by silver hake (*Merluccius bilinearis*) from the south coast of Newfoundland, Canada. *Marine Pollution Bulletin* 131, 267-275.

Lin, L., Ma, L. S., Li, H. X., Pan, Y. F., Liu, S., Zhang, L., Peng, J. P., Fok, L., Xu, X. R., & He, W. H. (2020). Low level of microplastic contamination in wild fish from an urban estuary. *Marine Pollution Bulletin* 160, 111650.

Lo, H. S., Lee, Y. K., Po, B. H. K., Wong, L. C., Xu, X., Wong, C. F., Wong, C. Y., Tam, N. F. Y., & Cheung, S. G. (2020). Impacts of Typhoon Mangkhut in 2018 on the deposition of marine debris and microplastics on beaches in Hong Kong. *Science of the Total Environment* 716, 137172.

Lo, H. S., Xu, X., Wong, C. Y., & Cheung, S. G. (2018). Comparisons of microplastic pollution between mudflats and sandy beaches in Hong Kong. *Environmental Pollution* 236, 208-217.

Löder, M. G. J., Kuczera, M., Mintenig, S., Lorenz, C., & Gerdts, G. (2015). Focal plane array detector-based micro-Fourier-transform infrared imaging for the analysis of microplastics in environmental samples. *Environmental Chemistry* 12, 563-581.

Lusher, A. L., Welden, N. A., Sobral, P., & Cole, M. (2017). Sampling, isolating and identifying microplastics ingested by fish and invertebrates. *Analytical methods* 9, 1346-1360.

Mai, L., Bao, L.-J., Shi, L., Wong, C. S., & Zeng, E. Y. (2018). A review of methods for measuring microplastics in aquatic environments. *Environmental Science and Pollution Research* 25, 11319-11332.

Mak, C. W., Tsang, Y. Y., Leung, M. M. L., Fang, J. K. H., & Chan, K. M. (2020). Microplastics from effluents of sewage treatment works and stormwater discharging into the Victoria Harbor, Hong Kong. *Marine Pollution Bulletin* 157, 111181.

Mendoza, L. M. R., Karapanagioti, H., & Álvarez, N. R. (2018). Micro(nanoplastics) in the marine environment: current knowledge and gaps. *Current Opinion in Environmental Science & Health* 1, 47-51.

Naidoo, T., Goordiyal, K., & Glassom, D. (2017). Are Nitric Acid (HNO 3) Digestions Efficient in Isolating Microplastics from Juvenile Fish?. *Water, Air, & Soil Pollution* 228, 1-11.

Naidu, S. A. (2019). Preliminary study and first evidence of presence of microplastics and colorants in green mussel, *Perna viridis* (Linnaeus, 1758), from southeast coast of India. *Marine Pollution Bulletin* 140, 416-422.

Naidu, S. A., Rao, V. R., & Ramu, K. (2018). Microplastics in the benthic invertebrates from the coastal waters of Kochi, Southeastern Arabian Sea. *Environmental Geochemistry and Health*, *40*, 1377-1383.

Nakajima, R., & Yamashita, R. (2020) Methods for sampling, processing, identification, and quantification of microplastics in the marine environment. *Oceanography in Japan* 29, 129-151 (in Japanese).

Nam, P. N., Tuan, P. Q., Thuy, D. T., & Amiard, F. (2019). Contamination of microplastic in bivalve: first evaluation in Vietnam. *Vietnam Journal of Earth Sciences* 41, 252-258.

Napper, I. E., & Thompson, R. C. (2016). Release of synthetic microplastic plastic fibres from domestic washing machines: Effects of fabric type and washing conditions. *Marine Pollution Bulletin* 112, 39-45.

Nava, V., & Leoni, B. (2020). A critical review of interactions between microplastics, microalgae and aquatic ecosystem function. *Water Research* 188, 116476.

Nelms, S. E., Galloway, T. S., Godley, B. J., Jarvis, D. S., & Lindeque, P. K. (2018). Investigating microplastic trophic transfer in marine top predators. *Environmental Pollution* 238, 999-1007.

Neves, D., Sobral, P., Ferreira, J. L., & Pereira, T. (2015). Ingestion of microplastics by commercial fish off the Portuguese coast. *Marine Pollution Bulletin* 101, 119-126.

Nie, H., Wang, J., Xu, K., Huang, Y., & Yan, M. (2019). Microplastic pollution in water and fish samples around Nanxun Reef in Nansha Islands, South China Sea. *Science of the Total Environment* 696, 134022.

Oßmann, B. E., Sarau, G., Schmitt, S. W., Holtmannspötter, H., Christiansen, S. H., & Dicke, W. (2017). Development of an optimal filter substrate for the identification of small microplastic particles in food by micro-Raman spectroscopy. *Analytical and Bioanalytical Chemistry* 409, 4099-4109.

Peez, N., Janiska, M. C., & Imhof, W. (2019). The first application of quantitative 1 H NMR spectroscopy as a simple and fast method of identification and quantification of microplastic particles (PE, PET, and PS). *Analytical and Bioanalytical Chemistry* 411, 823-833.

Peters, C. A., Hendrickson, E., Minor, E. C., Schreiner, K., Halbur, J., & Bratton, S. P. (2018). Pyr-GC/MS analysis of microplastics extracted from the stomach content of benthivore fish from the Texas Gulf Coast. *Marine Pollution Bulletin* 137, 91-95.

Phuong, N. N., Poirier, L., Pham, Q. T., Lagarde, F., & Zalouk-Vergnoux, A. (2018). Factors influencing the microplastic contamination of bivalves from the French Atlantic coast: location, season and/or mode of life?. *Marine Pollution Bulletin* 129, 664-674.

Phuong, N. N., Zalouk-Vergnoux, A., Kamari, A., Mouneyrac, C., Amiard, F., Poirier, L., & Lagarde, F. (2018). Quantification and characterization of microplastics in blue mussels (*Mytilus edulis*): protocol setup and preliminary data on the contamination of the French Atlantic coast. *Environmental Science and Pollution Research* 25, 6135-6144.

Pinto, R., Acosta, V., Segnini, M. I., Brito, L., & Martínez, G. (2015). Temporal variations of heavy metals levels in *Perna viridis*, on the Chacopata-Bocaripo lagoon axis, Sucre State, Venezuela. *Marine Pollution Bulletin* 91, 418-423.

PlasticsEurope (2019). Plastics—The Facts 2019. *An analysis of European plastics production, demand and waste data*, 1-42

Pozo, K., Gomez, V., Torres, M., Vera, L., Nuñez, D., Oyarzún, P., Mendoza, G., Clarke, B., Fossi, M. C., Baini, M., Přibylová, P. & Klánová, J. (2019). Presence and characterization of microplastics in fish of commercial importance from the Biobío region in central Chile. *Marine Pollution Bulletin*, *140*, 315-319.

Qiu, Q., Tan, Z., Wang, J., Peng, J., Li, M., & Zhan, Z. (2016). Extraction, enumeration and identification methods for monitoring microplastics in the environment. *Estuarine, Coastal and Shelf Science* 176, 102-109.

Qu, X., Su, L., Li, H., Liang, M., & Shi, H. (2018). Assessing the relationship between the abundance and properties of microplastics in water and in mussels. *Science of the Total Environment* 621, 679-686.

Railo, S., Talvitie, J., Setälä, O., Koistinen, A., & Lehtiniemi, M. (2018). Application of an enzyme digestion method reveals microlitter in *Mytilus trossulus* at a wastewater discharge area. *Marine Pollution Bulletin* 130, 206-214.

Reguera, P., Viñas, L., & Gago, J. (2019). Microplastics in wild mussels (*Mytilus* spp.) from the north coast of Spain. *Scientia Marina* 83, 337-347.

Renzi, M., Guerranti, C., & Blašković, A. (2018). Microplastic contents from maricultured and natural mussels. *Marine Pollution Bulletin* 131, 248-251.

Roch, S., & Brinker, A. (2017). Rapid and efficient method for the detection of microplastic in the gastrointestinal tract of fishes. *Environmental Science & Technology* 51, 4522-4530.

Roditi, H. A., Fisher, N. S., & Sañudo-Wilhelmy, S. A. (2000). Field testing a metal bioaccumulation model for zebra mussels. *Environmental Science & Technology* 34, 2817-2825.

Ronkay, F., Molnar, B., Gere, D., & Czigany, T. (2020). Plastic waste from marine environment: Demonstration of possible routes for recycling by different manufacturing technologies. *Waste Management* 119, 101-110.

Ryan, P. G., & Moloney, C. L. (1990). Plastic and other artefacts on South African beaches: Temporal trends in abundance and composition. *South African Journal of Science* 86, 450-452.

Santillo, D., Miller, K., & Johnston, P. (2017). Microplastics as contaminants in commercially important seafood species. *Integrated Environmental Assessment and Management* 13, 516-521.

Santos, J., Pham, A., Stasinopoulos, P., & Giustozzi, F. (2021). Recycling waste plastics in roads: A life-cycle assessment study using primary data. *Science of the Total Environment* 751, 141842.

Sathish, M. N., Jeyasanta, I., & Patterson, J. (2020). Occurrence of microplastics in epipelagic and mesopelagic fishes from Tuticorin, Southeast coast of India. *Science of the Total Environment* 720, 137614.

Sathish, M. N., Jeyasanta, K. I., & Patterson, J. (2020). Monitoring of microplastics in the clam *Donax cuneatus* and its habitat in Tuticorin coast of Gulf of Mannar (GoM), India. *Environmental Pollution* 266, 115219.

Savoca, S., Capillo, G., Mancuso, M., Bottari, T., Crupi, R., Branca, C., Romano, V., Faggio, C., D'Angelo, G., & Spanò, N. (2019). Microplastics occurrence in the Tyrrhenian waters and in the gastrointestinal tract of two congener species of seabreams. *Environmental Toxicology and Pharmacology* 67, 35-41.

Scott, N., Porter, A., Santillo, D., Simpson, H., Lloyd-Williams, S., & Lewis, C. (2019). Particle characteristics of microplastics contaminating the mussel *Mytilus edulis* and their surrounding environments. *Marine Pollution Bulletin* 146, 125-133.

Shim, W. J., Hong, S. H., & Eo, S. E. (2017). Identification methods in microplastic analysis: a review. *Analytical Methods* 9, 1384-1391.

Sin, S. N., Chua, H., & Lo, W. (2003). Sediment oxygen demand and nutrient balance in Tolo Harbour, a land-locked embayment in Hong Kong. In: Brebbia, C. A. (Ed.), *Transactions on Ecology and the Environment* 61. WIT Press, Southampton, pp. 217-223.

Sobhani, Z., Al Amin, M., Naidu, R., Megharaj, M., & Fang, C. (2019). Identification and visualisation of microplastics by Raman mapping. *Analytica Chimica Acta* 1077, 191-199.

Stock, F., Kochleus, C., Bänsch-Baltruschat, B., Brennholt, N., & Reifferscheid, G. (2019). Sampling techniques and preparation methods for microplastic analyses in the aquatic environment–A review. *TrAC Trends in Analytical Chemistry* 113, 84-92.

Stuart BH (2002) *Polymer analysis*, John Wiley and Sons, Chichester, 304 pp.

Su, L., Deng, H., Li, B., Chen, Q., Pettigrove, V., Wu, C., & Shi, H. (2019). The occurrence of microplastic in specific organs in commercially caught fishes from coast and estuary area of east China. *Journal of Hazardous Materials* 365, 716-724.

Sun, R., Yu, J., Liao, Y., Chen, J., Wu, Z., & Mai, B. (2020). Geographical distribution and risk assessment of dichlorodiphenyltrichloroethane and its metabolites in *Perna viridis* mussels from the northern coast of the South China Sea. *Marine Pollution Bulletin* 151, 110819.

Sun, X., Li, Q., Shi, Y., Zhao, Y., Zheng, S., Liang, J., Liu, T., & Tian, Z. (2019). Characteristics and retention of microplastics in the digestive tracts of fish from the Yellow Sea. *Environmental Pollution* 249, 878-885.

Tantanasarit, C., Babel, S., Englande, A. J., & Meksumpun, S. (2013). Influence of size and density on filtration rate modeling and nutrient uptake by green mussel (*Perna viridis*). *Marine Pollution Bulletin* 68, 38-45.

Teng, J., Wang, Q., Ran, W., Wu, D., Liu, Y., Sun, S., Liu, H., Cao, R., & Zhao, J. (2019). Microplastic in cultured oysters from different coastal areas of China. *Science of the Total Environment* 653, 1282-1292.

Thakur, S., Verma, A., Sharma, B., Chaudhary, J., Tamulevicius, S., & Thakur, V. K. (2018). Recent developments in recycling of polystyrene based plastics. *Current Opinion in Green and Sustainable Chemistry* 13, 32-38.

Thiele, C. J., Hudson, M. D., & Russell, A. E. (2019). Evaluation of existing methods to extract microplastics from bivalve tissue: Adapted KOH digestion protocol improves filtration at single-digit pore size. *Marine Pollution Bulletin* 142, 384-393.

Thompson, R. C., Olsen, Y., Mitchell, R. P., Davis, A., Rowland, S. J., John, A. W. G., McGonigle, D., & Russell, A. E. (2004). Lost at sea: where is all the plastic?. *Science(Washington)* 304, 838.

To, A., & Cheung, C.W. (2016). *The Sustainable Seafood Movement in Hong Kong*, World Wide Fund for Nature Hong Kong, 32 pp.

Tomás, J., Guitart, R., Mateo, R., & Raga, J. A. (2002). Marine debris ingestion in loggerhead sea turtles, *Caretta caretta*, from the Western Mediterranean. *Marine Pollution Bulletin* 44, 211-216.

Tsang, Y. Y., Mak, C. W., Liebich, C., Lam, S. W., Sze, E. T., & Chan, K. M. (2017). Microplastic pollution in the marine waters and sediments of Hong Kong. *Marine Pollution Bulletin* 115, 20-28.

Tuschel, D. (2016). Selecting an excitation wavelength for Raman spectroscopy. *Spectroscopy* 31,14-23

Valente, T., Sbrana, A., Scacco, U., Jacomini, C., Bianchi, J., Palazzo, L., de Lucia, G. A., Silvestri, C., & Matiddi, M. (2019). Exploring microplastic ingestion by three deep-water elasmobranch species: A case study from the Tyrrhenian Sea. *Environmental Pollution* 253, 342-350.

Van Cauwenberghe, L., & Janssen, C. R. (2014). Microplastics in bivalves cultured for human consumption. *Environmental Pollution* 193, 65-70.

Van Cauwenberghe, L., Claessens, M., Vandegehuchte, M. B., & Janssen, C. R. (2015). Microplastics are taken up by mussels (*Mytilus edulis*) and lugworms (*Arenicola marina*) living in natural habitats. *Environmental Pollution* 199, 10-17.

Verla, A. W., Enyoh, C. E., Verla, E. N., & Nwarnorh, K. O. (2019). Microplastic–toxic chemical interaction: a review study on quantified levels, mechanism and implication. *SN Applied Sciences* 1, 1-30.

Verlaan, M. P., Banta, G. T., Khan, F. R., & Syberg, K. (2019). Abundance of microplastics in the gastrointestinal tracts of the eelpout (*Zoacres viviparous* L.) collected in Roskilde Fjord, Denmark: Implications for use as a monitoring species under the Marine Strategy Framework Directive. *Regional Studies in Marine Science* 32, 100900.

von Friesen, L. W., Granberg, M. E., Hassellöv, M., Gabrielsen, G. W., & Magnusson, K. (2019). An efficient and gentle enzymatic digestion protocol for the extraction of microplastics from bivalve tissue. *Marine Pollution Bulletin* 142, 129-134.

Wagner, M., Scherer, C., Alvarez-Muñoz, D., Brennholt, N., Bourrain, X., Buchinger, S., Fries, E., Grosbois, C., Klasmeier, J., Marti, T., Rodriguez-Mozaz, S., Urbatzka, R., Vethaak, A. D., Winther-Nielsen, M., & Reifferscheid, G. (2014). Microplastics in freshwater ecosystems: what we know and what we need to know. *Environmental Sciences Europe* 26, 1-9.

Wakkaf, T., El Zrelli, R., Kedzierski, M., Balti, R., Shaiek, M., Mansour, L., Tlig-Zouari, S., Bruzaud, S., & Rabaoui, L. (2020). Microplastics in edible mussels from a southern Mediterranean lagoon: Preliminary results on seawater-mussel transfer and implications for environmental protection and seafood safety. *Marine Pollution Bulletin* 158, 111355.

Wang, C., Zhao, J., & Xing, B. (2020). Environmental source, fate, and toxicity of microplastics. *Journal of Hazardous Materials*, 124357.

Waring, R. H., Harris, R. M., & Mitchell, S. C. (2018). Plastic contamination of the food chain: A threat to human health?. *Maturitas* 115, 64-68.

Webb, S., Ruffell, H., Marsden, I., Pantos, O., & Gaw, S. (2019). Microplastics in the New Zealand green lipped mussel *Perna canaliculus*. *Marine Pollution Bulletin* 149, 110641.

Wobbrock, J. O., Findlater, L., Gergle, D., & Higgins, J. J. (2011, May). The aligned rank transform for nonparametric factorial analyses using only anova procedures. In *Proceedings of The SIGCHI Conference on Human Factors in Computing Systems* (pp. 143-146).

Wright, S. L., & Kelly, F. J. (2017). Plastic and human health: a micro issue? *Environmental Science & Technology* 51, 6634-6647.

Wu, P., Tang, Y., Dang, M., Wang, S., Jin, H., Liu, Y., Jing, H., Zheng, C., Yi, S., & Cai, Z. (2020). Spatial-temporal distribution of microplastics in surface water and sediments of Maozhou River within Guangdong-Hong Kong-Macao Greater Bay Area. *Science of the Total Environment* 717, 135187.

Xanthos, D., & Walker, T. R. (2017). International policies to reduce plastic marine pollution from single-use plastics (plastic bags and microbeads): a review. *Marine Pollution Bulletin* 118, 17-26.

Xiong, X., Zhang, K., Chen, X., Shi, H., Luo, Z., & Wu, C. (2018). Sources and distribution of microplastics in China's largest inland lake–Qinghai Lake. *Environmental Pollution* 235, 899-906.

Xu, J. L., Thomas, K. V., Luo, Z., & Gowen, A. A. (2019). FTIR and Raman imaging for microplastics analysis: State of the art, challenges and prospects. *TrAC Trends in Analytical Chemistry* 119, 115629.

Xu, X. Y., Wong, C. Y., Tam, N. F. Y., Liu, H. M., & Cheung, S. G. (2020). Barnacles as potential bioindicator of microplastic pollution in Hong Kong. *Marine Pollution Bulletin* 154, 111081.

Xu, X., Wong, C. Y., Tam, N. F., Lo, H. S., & Cheung, S. G. (2020b). Microplastics in invertebrates on soft shores in Hong Kong: Influence of habitat, taxa and feeding mode. *Science of the Total Environment* 715, 136999.

Yeung, J. W., Zhou, G. J., & Leung, K. M. (2017). Spatiotemporal variations in metal accumulation, RNA/DNA ratio and energy reserve in *Perna viridis* transplanted along a marine pollution gradient in Hong Kong. *Marine Pollution Bulletin* 124, 736-742.

Zhang, C., Wang, S., Pan, Z., Sun, D., Xie, S., Zhou, A., Wang, J. & Zou, J. (2020). Occurrence and distribution of microplastics in commercial fishes from estuarine areas of Guangdong, South China. *Chemosphere* 260, 127656.

Zhang, F., Wang, X., Xu, J., Zhu, L., Peng, G., Xu, P., & Li, D. (2019). Food-web transfer of microplastics between wild caught fish and crustaceans in East China Sea. *Marine Pollution Bulletin* 146, 173-182.

Zhang, K., Hamidian, A. H., Tubic, A., Zhang, Y., Fang, J. K-H., Wu, C., & Lam, P. K. S. (2021) Understanding plastic degradation and microplastic formation in the environment: a review. *Environmental Pollution* 274, 116554.

Zhang, X., Yan, B., & Wang, X. (2020). Selection and optimization of a protocol for extraction of microplastics from *Mactra veneriformis*. *Science of The Total Environment* 746, 141250.

Zhao, Y., Sun, X., Li, Q., Shi, Y., Zheng, S., Liang, J., Liu, T., & Tian, Z. (2019). Data on microplastics in the digestive tracts of 19 fish species from the Yellow Sea, China. *Data in Brief* 25, 103989.

Zhu, J., Zhang, Q., Li, Y., Tan, S., Kang, Z., Yu, X., Lan, W., Wang, J., & Shi, H. (2019). Microplastic pollution in the Maowei Sea, a typical mariculture bay of China. *Science of the Total Environment* 658, 62-68.

Zhu, L., Wang, H., Chen, B., Sun, X., Qu, K., & Xia, B. (2019). Microplastic ingestion in deep-sea fish from the South China Sea. *Science of the Total Environment* 677, 493-501.